The isotopic composition of CO in car exhaust

Master's thesis

Author:
Stijn Naus

Supervisors:
Dr. M. E. Popa
Prof. dr. T. Röckmann

Institute of Marine and Atmospheric research Utrecht
University of Utrecht

July 1, 2016

Abstract

In this study, the isotopic composition of CO and of CO_2 and the CO:CO_2, CH_4:CO_2 and H_2:CO gas ratios in the exhaust of individual cars were investigated. This was done under idling and revving conditions, and for three cars in a full driving cycle on a test bench. The spread in the results, even within a single car, was large: for δ^{13}C in CO $\sim$ 0 to -60 ‰, for δ^{18}O in CO $\sim$ +20 to +35 ‰, and for all gas ratios several orders of magnitude. The results show an increase in the spread of isotopic values for CO compared to previous studies, suggesting that increasing complexity of emission regulations in cars might be reflected in the isotopic composition. When including all samples, we find a weighted mean for the δ^{13}C and δ^{18}O in CO of -28.7 $\pm$ 0.5 ‰ and 24.8 $\pm$ 0.3 ‰ respectively. This result is dominated by cold petrol cars. Our results suggest that in driving cycles where cold emissions are less important, both δ^{13}C and δ^{18}O would be expected to increase, which would result in isotopic values more in line with previous studies.

For the H_2:CO ratio, averaged over all cars, we found a value of 0.71 $\pm$ 0.31 ppb:ppb, in agreement with previous literature. The CO:CO_2 ratio, with a mean of 19.4 $\pm$ 6.8 ppb:ppm, and the CH_4:CO_2 ratio, with a mean of 0.26 $\pm$ 0.05 ppb:ppm, are both higher than is reported in recent literature. This is likely because our sampling distribution was biased towards cold cars, and therefore towards higher emission situations. In many ways the CH_4:CO_2 ratio was found to behave similarly to the CO:CO_2 ratio, suggesting that the processes affecting CO and CH_4 are similar.

Diesel cars behaved as a distinct group, with CO enriched in ^{13}C and depleted in ^{18}O compared to petrol cars. CO emissions from cold diesel cars were found to be significant, but reduced sharply in hot diesel cars.

The δ^{13}C values in CO_2 were close to the δ^{13}C expected from fuel, with no significant difference between petrol and diesel cars. The δ^{18}O values in CO_2 for petrol cars covered a range of 20 to 35 ‰, similar to the δ^{18}O of CO. The δ^{18}O values in CO_2 for diesel cars were closely centred around the δ^{18}O in atmospheric oxygen.

A set of samples taken in and near several parking garages showed good agreement with the individual car measurements. A δ^{13}C of -29.5 $\pm$ 0.4 ‰, a δ^{18}O of 25.9 $\pm$ 0.4 ‰(both for CO) and a H_2:CO ratio of 0.46 $\pm$ 0.06 ppb:ppm were found. This shows that, at least in parking garages, cold idling emissions play an important role.

Contents

1 Introduction

1.1 CO emissions from traffic

Carbon monoxide (CO) plays an important role in the atmosphere. CO occupies a large part ($\sim$ 60 % (Crutzen and Zimmermann, 1991)) of the cleaning capacity of the hydroxyl-radical (OH). OH, also known as the cleaning detergent of the atmosphere, oxidises reduced and partly oxidized compounds such as nitrogen oxides, methane and other hydrocarbons. Therefore, if the CO burden on OH increases, less OH will be available for reaction with other pollutants, which can indirectly lead to i.a. increased global warming. In addition CO can act as an ozone precursor, thus enhancing the already significant dangers of ozone smog in urban areas.

An estimate of the global CO budget is given in Table 1 (Brenninkmeijer et al., 1999). Overall CO has a lifetime in the order of months, which means it is long-lived enough to be influenced by transport, but short-lived enough not to be well-mixed globally. Therefore in most areas atmospheric CO is made up of a background level, combined with a contribution of local sources. In different areas different sources from the global CO budget will dominate. Generally in the Southern Hemisphere biomass burning is especially important, whereas in the Northern Hemisphere, even more so in urban areas, anthropogenic sources are more important.

Source	Magnitude (Tg/yr)
Fossil fuel combustion	300-550
Biomass burning	300-700
CH_4 oxidation	400-1000
NMHC oxidation	200-600
Ozonolysis	80-100
Biogenic	60-160
Oceans	20-200
Total sources	1800-2700

Sink	Magnitude (Tg/yr)
Oxidation by OH	1400-2600
Soil uptake	250-640
Loss to stratosphere	$\sim$100
Total sinks	2100 - 3000

Table 1: The global tropospheric budget of CO (Brenninkmeijer et al., 1999).

The main anthropogenic source of CO in urban areas is fossil fuel burning, to which an important contribution is given by traffic. Since a large part of the world population lives in urban areas, it is vital to understand these traffic emissions. The density of traffic in most areas has been growing over the past few decades. On the other hand, emissions per car, especially non-CO_2 emissions, have been decreasing, due to a number of technological innovations (see section 1.2). There are indications that this has lead to a continuous decrease in CO emissions from road transport since 1990 (e.g. EC-JRC/PBL.

EDGAR version 4.0., 2009), but traffic is still an important contributor. This study will focus on CO emissions from passenger cars: the main body of most traffic fleets.

1.2 Relevant vehicle characteristics

Since the focus of this study lies on emissions from passenger cars, it is useful to explain some of their general properties. There are few important aspects to car mechanics that will be relevant to this study. The first is fuel type. Most cars either run on diesel or petrol, which are both driven by an internal combustion engine. Such an engine works through explosive ignition of fossil fuel. The difference between petrol and diesel is that in petrol engines an air-fuel mixture is spark-ignited. In diesel engines only air is taken in. The air is then compressed, after which fuel is injected. Because of the strong compression, the fuel is instantly ignited.

A petrol car aims to run at the stoichiometric point, where the amount of oxygen introduced into the engine is exactly enough to burn all fuel introduced into the engine. However, quick changes, such as rapid acceleration, can push petrol engines away from the stoichiometric point. Diesel engines burn lean, i.e. with an excess of oxygen. This is more fuel efficient but also leads to increased emissions of NO_x. Lean burning reduces CO emissions, since there is always an excess of oxygen available at the time of ignition.

In petrol cars the combustion is quite incomplete and CO output of the engine can be high. For this reason catalytic converters were introduced, which convert the most important toxic pollutants to less toxic pollutants. These were first widely implemented in the 1990s and currently almost every petrol car is equipped with a three-way catalytic converter (TWC). A TWC oxides CO and hydrocarbons to CO_2 and H_2O and reduces NO_x to N_2 and O_2. An optimally functioning, modern TWC can reduce CO from up to a few hundred ppm to levels below atmospheric, though a TWC wears with age (Andersson et al., 2007). However, in practice a TWC may not always perform at optimal efficiency.

Most importantly, a TWC has to be sufficiently heated to function. Though progress has been made in pre-heating TWCs, in nearly all cars the TWC is still heated indirectly by air from the engine. Pollutants emitted before the TWC is sufficiently heated, are called cold-start extra emissions (CSEE). CSEE have been subject to a relatively large number of studies, because they may provide a large contribution to emissions of non-CO_2 emissions, such as CO (e.g. Bielaczyc et al. (2011); Weiss et al. (2011)). Especially in urban areas, where short trips are common, CSEE can dominate CO emissions (Weilenmann et al., 2009). These emissions are not easy to quantify, since they strongly depend on ambient temperature (Ludykar et al. (1999); Weilenmann et al. (2005)), the type of driving cycle (Weilenmann et al., 2005) and the age of the car (Weilenmann et al., 2005). In addition, even a properly heated TWC functions sub-optimal, when the engine does not burn at the stoichiometric point, for example because of rapid acceleration. Though there is an oxygen buffer included in modern TWCs to reduce this effect, there are limits to its efficiency.

These deviations from optimal performance only occur for a relatively short period, but because of the high optimal efficiency of TWCs emissions, they can certainly be significant. Similarly, a few cars driving around with a malfunctioning TWC can emit the equivalent of a large number of properly working cars. These problems may skew the distribution of CO emissions towards a small number of cars and/or driving conditions.

Any research project into CO should consider these complications.

Diesel cars have different issues. Because a diesel engine burns lean, too much oxygen is present in the exhaust gas to effectively reduce NO_x to N_2 and O_2 using a TWC. A diesel catalytic converter only oxidises CO and hydrocarbons, but does not reduce NO_x levels. For this reason a technique called exhaust gas recirculation (EGR) is used in diesel cars. Up to 50% of the exhaust gas is re-introduced into the engine to reduce NO_x emissions. EGR is also used in petrol engines, though only 5-15% of exhaust gas is recirculated. Depending on the driving conditions, EGR can both increase and reduce fuel efficiency and toxic emissions, so that EGR is only turned on under a specific set of conditions.

These characteristics show that reducing pollutant emissions from vehicles can be done in several ways, increasing optimal catalytic efficiency not necessarily being the best of them. Since car manufacturers tend to be secretive about the exact implementations of the various techniques (e.g. EGR), it is not always possible to get quantitative insight into a car's chemistry. However, knowing the choices available to manufacturers will already be useful in interpreting any results.

1.3 Isotopes

This study is aimed at determining the isotopic composition of CO in car exhaust, which can help in using isotopes to track CO emissions from traffic. Isotopes are atoms with the same number of protons, but a different number of neutrons and thus a different mass. Similarly, isotopologues are molecules with a the same number of protons, but a different number of neutrons. Isotopes will be denoted as ^{x}Y, with x the mass and Y the atom name. Isotopes of the same element can differ in nuclear properties (e.g. stable/unstable), but are chemically largely indistinguishable.

Because both the relative abundance of secondary isotopes and the variations in their abundance are generally low, abundances are not expressed in absolute terms but in the relative δ-value. This value quantifies enrichment or depletion relative to a standard ratio of known composition. It is defined as:

$$\delta = (\frac{R_{sample}}{R_{reference}} - 1) \cdot 1000‰, \tag{1}$$

where R is the ratio between the abundance of the isotope of interest and that of the most abundant isotope. The isotopes relevant to this paper are ^{13}C (relative to ^{12}C) and ^{18}O (relative to ^{16}O). For both ^{13}C and ^{18}O an international standard ratio exists, allowing comparison between different laboratories. For ^{13}C the standard is Vienna Pee Dee Belemnite (VPDB) and for ^{18}O it is Vienna Standard Mean Ocean Water (VSMOW).

Since different sources often emit chemicals with different isotopic compositions, isotopes can be used for improving atmospheric budgets. When both the isotopic signature of the sources and that of the atmosphere are known, then the relative contribution of each source can be quantified. Limitations are that the isotopic source signatures need to be sufficiently distinct and that only $n+1$ sources can be identified, with n the number of available isotopes. Additionally, sinks can affect the isotopic composition, so that these processes also have to be sufficiently understood.

Source	δ^{13}C (‰)	δ^{18}O (‰)
Fossil fuel combustion	-27.5	23.5
Biomass burning	-22.9	17.2
CH_4 oxidation	-51.1	0
NMHC oxidation	-32.2	0
Atmospheric comp.	-28 to -23	0 to 10

Table 2: The isotopic composition emitted by the most important CO sources, along with the isotopic composition of CO in the atmosphere. (Röckmann et al., 2002)

1.4 The isotopic composition of CO

An overview of the isotopic signatures of the different CO sources is given in Table 2. The atmospheric composition is also given. The different sources have distinct isotopic signatures, which makes them useful in tracing CO emissions.

Research into the isotopic signature of CO from traffic is limited. Generally it is considered that the δ^{13}C values of CO in car exhaust reflect those of the fossil fuel ($\sim$ -26 to -30 ‰ (Andres et al., 1994)), depending on the oil source) that is burned. For CO emitted by gasoline cars, δ^{13}C values around -23 to -30 ‰ have been found (Stevens et al. (1972); Brenninkmeijer and Röckmann (1997); Kato et al. (1999); Tsunogai et al. (2003)). For diesel cars values of -19.5 $\pm$ 0.7 ‰(Tsunogai et al., 2003) and -22.2 ‰ (Kato et al., 1999) have been reported . The oxygen in CO from car exhaust originates from atmospheric oxygen, but δ^{18}O values for gasoline CO have been reported in a range of 20-26 ‰. For diesel δ^{18}O values are more depleted towards 10-20 ‰. In a recent tunnel study (Popa et al., 2014), the isotopic composition of traffic CO was estimated as δ^{13}C = -25.6 $\pm$ 0.2 ‰ and δ^{18}O = 24.1 $\pm$ 0.2 ‰. These estimates of the isotopic composition of traffic CO show that the δ^{13}C value of traffic is close to atmospheric, but the δ^{18}O value is much higher than atmospheric, so that CO emissions from traffic would especially affect δ^{18}O values in the atmosphere.

All studies that investigate CO isotopologues from traffic follow one of two approaches. Firstly there are studies in which the exhaust composition of individual cars is measured. The difficulty with this approach is that measurements are time-consuming, so that only a small number of cars can be measured (Brenninkmeijer and Röckmann (1997): 1 car; Kato et al. (1999): 4 cars; Tsunogai et al. (2003): 6 cars). Moreover, in only one study (Tsunogai et al., 2003) a full driving cycle was simulated. The other studies only considered idling cars or cars for which the accelerator was pressed without coupling (revving). Given the problems with car studies outlined in section 1.2 and the strong temporal variations of the CO isotopic composition from cars under different driving conditions (Tsunogai et al., 2003), such small numbers of cars cannot directly be extrapolated to represent the average car. Even if this were possible, the average car is not necessarily the most important CO emitter.

In the second approach samples are taken from highly polluted locations, mainly tunnels or highways (Stevens et al. (1972); Kato et al. (1999); Popa et al. (2014)), so that a result integrated over a number of cars and driving conditions is obtained. This type of study generally provides precise and reproducible estimates. However, there might be

a bias towards a restricted number of driving conditions (e.g. no CSEEs for tunnels). Moreover, no insight is obtained into the most important contributors to traffic CO, both in terms of driving conditions and of differences between cars. This means that the results can't be extrapolated to other countries where the traffic fleet composition is different. In addition, it does not allow to identify and reduce the important contributors to traffic CO.

Regardless of these issues, studies into CO isotopes from traffic are few and sparsely spread through time. Given the rapidly innovating nature of the car industry, it is not even certain whether they can be compared. For example, the measurements done in Stevens et al. (1972) took place before the introduction of TWCs. Such a strong alteration of car chemistry is likely to have introduced a change in CO composition from cars.

1.5 Gas ratios

Gas ratios can also be used for estimating contributions from individual sources to changes in the atmosphere, complementary to isotope measurements. Similarly to isotopes, most sources will emit gases in different ratios. When a deviation from background concentrations is measured in the atmosphere, then the ratio between the deviations of different gases can provide information on the source. Since gas concentrations are easier to measure than isotopes, there are more results available for gas ratios in car exhaust. On the other hand, the tracer for one gas is coupled to a second gas, so that it is more likely deviations are caused by more than one source or sink. In this study the gas ratios H_2:CO, CO:CO_2 and CH_4:CO_2 were measured.

The CO:CO_2 ratio is measured to allow comparison between different cars and studies, since absolute CO concentrations can be influenced by the exact sampling approach and by dilution of the exhaust air. Since nearly all carbon is emitted by a car as CO_2, expressing any emission relative to CO_2 emissions is analogous to expressing emissions relative to the amount of fuel burnt. Additionally, the CO:CO_2 ratio may provide a cheap and easy method for determining CO_2 emissions from fossil fuels, complementary to ^{14}C tracing (Gamnitzer et al., 2006). For petrol cars, values in the range of 5-50 mmol mol^{-1} have been reported (e.g. Frey et al. (2003); Guo et al. (2006); Pelkmans and Debal (2006)). For diesel, some studies report emissions around 25-50% of what is found for petrol cars (Vollmer et al. (2007); Grant et al. (2010)), while others estimate it in the range of only a few percent (Bond et al., 2010). For overall traffic, recently reported values cover a range of 4 to 9 mmol mol^{-1} (Vollmer et al. (2007); Bishop and Stedman (2008); Popa et al. (2014)).

The main use of the H_2:CO ratio is deducing H_2 traffic emissions from the CO budget, since the H_2 budget itself is poorly constrained (Hammer et al., 2009). Moreover, since it is understood that TWCs oxidise CO more efficiently than H_2, the ratio is expected to increase when catalytic efficiency increases. Widely varying values have been reported for individual gasoline cars: the total range reported in studies spans 0.4−5.7 mol mol^{-1} (e.g. Bond et al. (2010); Vollmer et al. (2010)). Most studies report a more constrained fleet averaged ratio of 0.4−0.6 mol mol^{-1} (Vollmer et al. (2007); Aalto et al. (2009); Yver et al. (2009); Grant et al. (2010); Popa et al. (2011)). For diesel vehicles H_2 emissions are generally considered to be insignificant.

The CH_4:CO_2 ratio can be used to quantify CH_4 emissions from traffic. Reported values of the CH_4:CO_2 range from $4.6 \cdot 10^{-2}$ (Popa et al., 2014) to 0.41 ppb:ppm (Nam et al., 2004). However, even the highest estimate shows that CH_4 emissions from cars are negligible in the overall budget.

2 Project outline

The project is focused on updating estimates of CO isotopes in car exhaust. Ideally, this would lead to a well-constrained $\delta^{13}C$ and $\delta^{18}O$ value for CO from traffic. More in general, the influence of driving conditions and of car characteristics on the isotopic composition of CO was studied. Since gas ratios were also measured, the influence of the same parameters on the three gas ratios H_2:CO, CO:CO_2 and CH_4:CO_2 was investigated as well. Of primary interest are the differences between diesel and petrol cars and those between hot and cold cars. When possible, the influence of velocity and acceleration will also be studied. Literature values for all parameters are summarized in Table 3.

The first part of the project focused on emissions from idling cars. This serves several purposes. Firstly, it is the easiest method to sample a large number of cars. It can therefore give a good indication of variations between cars. Additionally, it provides information on the influence of car characteristics and on the difference in emissions between hot and cold cars. The final reason is one of convenience. Idling samples are easily obtained by sampling cars in parking lots. Since sampling is quick (see section 3.1), volunteers were abundant. This allowed familiarization with the measurements instruments and optimization of the sampling approach, without worrying about losing many samples.

For the second part, I took samples from cars placed on a test bench. On the test bench the influence of a select set of driving conditions was investigated. Since it was only possible to measure on a test bench for one day, full driving conditions could only be investigated for three cars.

The third part is intended as a intermediary between the first two parts. Cars of volunteers were measured stationary (i.e. de-coupled), but with the accelerator pressed to a varying number of rounds per minute (rpm). This allowed more detailed measurements of individual cars compared to the idling measurements, but it was easier to organise than measurements on a test bench. Additionally, this is how emissions are tested in the Dutch APK test. The APK test is the test that every Dutch car has to undergo every few years. Since this is the only emission test to which Dutch cars have to comply after leaving the factory, it will be interesting to see if they give an accurate representation of actual emissions. These measurements are referred to as revving.

Finally, I took samples in a number of parking garages. From these samples a source signature averaged over a large number of cars was estimated, both for isotopes and for the gas ratios. These results help in putting the individual car measurements in context.

The overall sample distribution is given in Table 4.

Parameter	Gasoline	Diesel
$\delta^{13}C$ (‰)	-23 to -30	-19 to -23
$\delta^{18}O$ (‰)	20 to 26	10 to 15
H_2:CO (ppb:ppb)	0.4 to 0.6	n.a.
CO:CO_2 (ppb:ppm)	5 to 50	0 to 20
CH_4:CO_2 (ppb:ppm)	$4.6 \cdot 10^{-2}$ to 0.41	

Table 3: Ranges reported in literature for the composition of car exhaust.

Measurement series	No. petrol cars	No. petrol samples		No. diesel cars	No. diesel samples	
		Hot	Cold		Hot	Cold
Parking lot	20	11	12	8	4	4
Test bench	3	56		0	0	
Revving	2	23		2	16	
Parking garage	25					

Table 4: The sampling distribution of the measurements in this study. Where possible a distinction between hot/cold and petrol/diesel cars was made. In total 126 samples were taken from 35 cars, in addition to the 25 background samples taken in and near parking garages.

3 Methods

3.1 Sampling

Accurate in situ measurement of CO and its isotopic composition is not possible, because of the low abundance of secondary isotopes and trace gases in general. Therefore obtaining results for car exhaust composition requires sampling of car air and subsequent analysis in the lab. This only works well, if the sample air is stable on the time scale in which measurements are done. A diagram of the sampling set-up is shown in Figure 1.

I took and stored the samples in glass flasks equipped with PCTFE seals, made by Normag, Ilmenau, Germany. These are designed to minimize reactions between the flask and greenhouse gases in the sample. For sampling, I first evacuated the flasks. Next I connected a drier and a particulate filter to the flask. The drier consists of a plastic tube filled with magnesium perchlorate (MgO), held in place by glass wool. I used a 7 micron stainless steel particulate filter. The samples were dried to prevent condensation inside the flask and to prevent any post-sampling reactions with water. Particulate matter was filtered to keep the flasks as clean as possible. To sample, I inserted a tube into the car tailpipe and opened the flask. The flask then filled to atmospheric pressure with exhaust

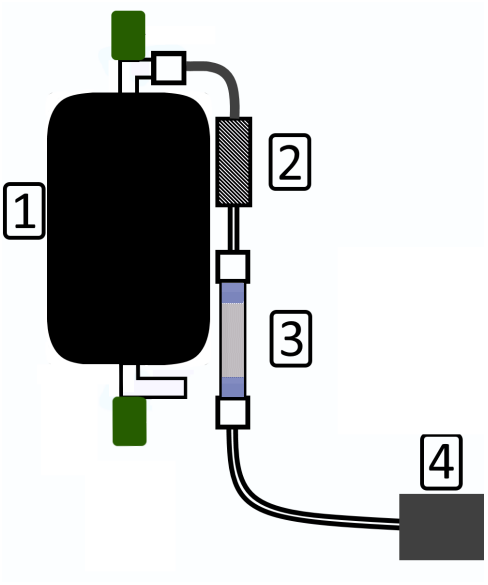

Figure 1: The sampling set-up used for sampling car exhaust: **1)** Flask, **2)** Particulate filter, **3)** Magnesium perchlorate drier, **4)** Car tailpipe.

air. The time it took for the flask to fill was around 25-35 seconds. Using a syringe, the sampling set-up was flushed with outside air, to avoid memory effects between samples.

3.2 Dilution and sample duplicates

Since the samples consisted mainly of car exhaust air, concentrations were generally too high to measure without additional dilution. Samples were diluted with CO-free synthetic air, which contained CO concentrations below the detection level of the RGA (< 10 ppb). For the dilution I used a system of stainless steel tubes to which a LEO-1 pressure sensor, a sample flask, a zero air cylinder and a vacuum pump were connected. The vacuum pump and the CO-free cylinder were connected with a switch valve so that either one or the other (or none) could be opened.

To dilute, I first evacuated the tube system. Next I opened the sample and reduced it to the desired pressure with the vacuum pump. Then I closed the flask again, evacuated the tube system and flushed it once with zero air. Then I opened the connection to the zero air cylinder, as well as the flask, and the flask pressure was increased to the required level. Depending on the flask's contents, they were diluted up to several tens of thousands of times.

The pressure sensor was calibrated at the start of the project (see Appendix A). This calibration showed that the sensor had an average offset of 0.7 mbar and, when corrected for this offset, an average error of 0.4 mbar. Since the pressure sensor is accurate to mbar, the instrumental error is estimated as 1.0 mbar. All pressure data was corrected for the offset.

Both as a precaution and as a way to quantify reproducibility of the entire measurement process, duplicates of some samples were made. This was done by connecting a flask to a different evacuated flask. The air from the sample flask was then split between the two flasks. There was no way to flush the connection, so that some background air

was added to both flasks. However, this was only a few ml and sample concentrations were generally so far above the background, that the effect on gas ratios and isotopes is deemed insignificant.

3.3 Measurement systems

3.3.1 Picarro

CO_2 and CH_4 concentrations were measured on a Picarro G2301 system. This is a continuous flow instrument, which analyses the air taken in based on its spectral absorption properties. It distinguishes between CO_2, CH_4 and H_2O. The gases are distinguished through their unique near-infrared absorption spectrum. Generally trace gases are present in low concentrations, so that they can not be measured directly through spectroscopy. In Picarro a cavity is filled with sample air. The cavity is defined by three mirrors. These mirrors are 99.999% reflective, so that they leak some light. A measurement is done by sending a single-frequency laser through the cavity. After the laser is shut off, the mirrors leak light, exponentially decaying to zero. Since the effective path-length is on the order of km, measuring the decay of the light and comparing it with the decay with no absorption present, gives the concentration of trace gases to high accuracy.

To measure on Picarro, I took air ($\sim$ 140 ml) from the sample flask by connecting it to a syringe with a septum. Due to overpressure in the flask, the syringe filled with sample air. I then similarly connected the syringe to Picarro, which evacuated the syringe. I measured each flask three times, to ensure reproducibility. Before each measurement the connection of the flask was flushed with sample air. Repeatibility of CO_2 and CH_4 were found to be 20 ppm and 20 ppb respectively, when measured in a range of 400-8000 ppm and 600-10000 ppb respectively. These errors were found to lead to a realistic analytical error in the end result (see Appendix B.

3.3.2 Reduced Gas Analyser

The H_2 and CO concentrations were measured using a Peak Performer 1 reduced gas analyser (RGA). In the RGA a sample loop is first flushed with sample air, after which sample air is collected in the loop. The loop is then flushed by a (non-H_2, non-CO) carrier gas, which carries the sample air into a molecular sieve. The molecular sieve slows down different gases at different rates, depending on the molecular mass. Because H_2 is lighter than CO, it will cross the sieve more quickly. The gas then arrives at a UV detector. The detector consists of solid HgO, which readily reacts with and, ideally, only with H_2 and CO, according to:

$$\mathrm{X} + \mathrm{HgO(s)} \rightarrow \mathrm{XO} + \mathrm{Hg(g)}. \tag{2}$$

This means that a certain amount of gaseous Hg is released, proportional to the concentration of H_2 or CO. This Hg moves into a compartment placed between a UV-light and a UV-detector, thus reducing the amount of light reaching the detector. This reduction is given as a voltage and can be translated into concentration levels through calibration with a reference gas of known composition. Because H_2 and CO arrive at the detector at different times, two distinct peaks are recorded.

I measured each sample three times and measured a known reference gas three times before and three times after the sample measurements. I linearly interpolated the reference voltages to the times of sample measurement and by comparing the two I deduced a sample concentration. The RGA may behave non-linearly, especially for high voltages. For this reason a non-linearity test was done. This showed that for optimal results, a non-linearity correction was needed (see Appendix C).

The instrumental error was estimated at 3 ppb for CO and 9 ppb for H_2. The non-linearity correction introduced an error of 1%. The uncertainty in the reference concentration introduced an error of 3%. These estimates were found to lead to realistic errors (see appendix B).

3.3.3 Continuous Flow Isotope Ratio Mass Spectrometer

Both CO and CO_2 isotopologues were measured using a measurement set-up based on a Continuous Flow Isotope Ratio Mass Spectrometer (CF-IRMS). The system consists of two parts. In the first part CO_2 is removed and CO is oxidised to CO_2. The second part is a mass spectroscope, which analyses the isotopic composition of this CO_2. The advantage of this conversion is that that most high-accuracy mass spectroscopy is based on CO_2 and that there is no interference between CO and N_2, which have the same mass,. The system used in this study, described in Pathirana et al. (2015), allows for quicker measurements and requires smaller sample sizes than is the case for similar systems that have been used before.

Eight samples and a reference gas can be connected simultaneously. Either a sample or the reference gas then enters the system. To measure CO isotopes the gas undergoes the following steps:

- T0: The gas enters a chemical trap with Ascarite, which absorbs the CO_2, and Magnesium Perchlorate, which dries the air.
- T1: The next step consists of a cryogenic trap, cooled by liquid nitrogen. Therefore gases that condense at liquid nitrogen temperatures (-196 ^{o}C), such as CO_2, condense and are removed.
- T2: The CO is then oxidized into CO_2 using the Schütze reagent. This reagent consists of I_2O_5 on granular silicon gel.
- T3: The gas is again cooled by liquid nitrogen. However, this time the condensed part is retained, which should now only contain CO_2.
- T4: Finally, the remaining now-CO_2 is moved into a small-diameter tube, which increases the pressure.

This entire system is continuously flushed with helium, which acts as a cleaning agent.

After these traps, the flow and gas concentrations are optimized for measurements in the IRMS in an open split. The split consists of a sample/reference capillary, a pure CO_2 capillary and a He capillary, which can each be lowered for different flows into the split. The air entering the split is pushed into a fourth capillary, which connects to the IRMS.

The flow from the pure CO_2 capillary, along with flow from the He capillary for dilution, is called the working gas.

To directly measure CO_2 isotopes, only trap T3 and T4 are used. However, the CF-IRMS is optimized to measure CO, which has a much lower abundance than CO_2. To measure atmospheric CO_2 levels a reduced volume of air is injected into the system and the air is additionally diluted in the split, by lowering the He capillary. Because of the continuous helium flushing, CO_2 concentrations entering the IRMS are them similar to what enters when CO isotopes are measured.

After the preparation the now-CO_2 enters the mass spectrometer. Since isotopes are chemically mostly identical, the technique for measuring isotopes distinguishes between them based on their mass. In a mass spectroscope all molecules are given a fixed electric charge. The molecules are then launched through a magnetic field, which will exert the same charge-based force on all molecules. The degree to which a molecule is deflected, is proportional to its mass. By counting how many molecules end up at certain positions, the relative abundance of each isotope can be determined.

For every sample run, there is a comparison with a known reference gas, measured before and after each sample set. The reference values are linearly interpolated to the times at which samples were measured. Both the samples and the reference runs are measured against the working gas, of which only the $\delta^{18}O$ value is needed for determining the $\delta^{18}O$ of the atom added in the Schütze reagent. In addition, blank runs are done and similarly interpolated, to quantify background CO_2 released by the Schütze reagent. Blank runs are done by measuring a closed in-take channel, so that no air is taken in.

The documented repeatability for the CO mole fraction is 0.7 %, for $\delta^{13}C$ it is 0.1 ‰ and for $\delta^{18}O$ it is 0.2 ‰ (Pathirana et al. (2015)). For our results, this was adjusted to 0.2 ‰ and 0.3 ‰ respectively (see section B). For both blank runs and runs with samples the system was found to behave linearly. Only when the integrated peaks were smaller than $\sim$ 5 Vs did non-linearity in the δ values occur. For this reason all samples were when possible measured with CO concentrations high enough to be in the linear range. Measurements with a peak height below 3 Vs were discarded.

3.4 Testbench

To investigate the influence of driving conditions on exhaust composition, a test bench was used. The test bench is made out of four sets of rollers. A car can be placed on the rollers and when the wheels roll, the rollers roll along with it to ensure the car doesn't move. In addition the car is strapped down, so that it can not shoot off the bench. An exhaust hood was placed near the car tailpipe to prevent toxic gas levels.

4 Results

4.1 Idling results

In total 58 samples were taken under idling conditions, from 35 different cars. Of these samples, 50 were measured for all gas concentrations and 45 for the isotopic composition of CO. Most idling samples were taken on a parking lot. Also included are the idling samples taken during the revving and testbench measurements. For each car the car type,

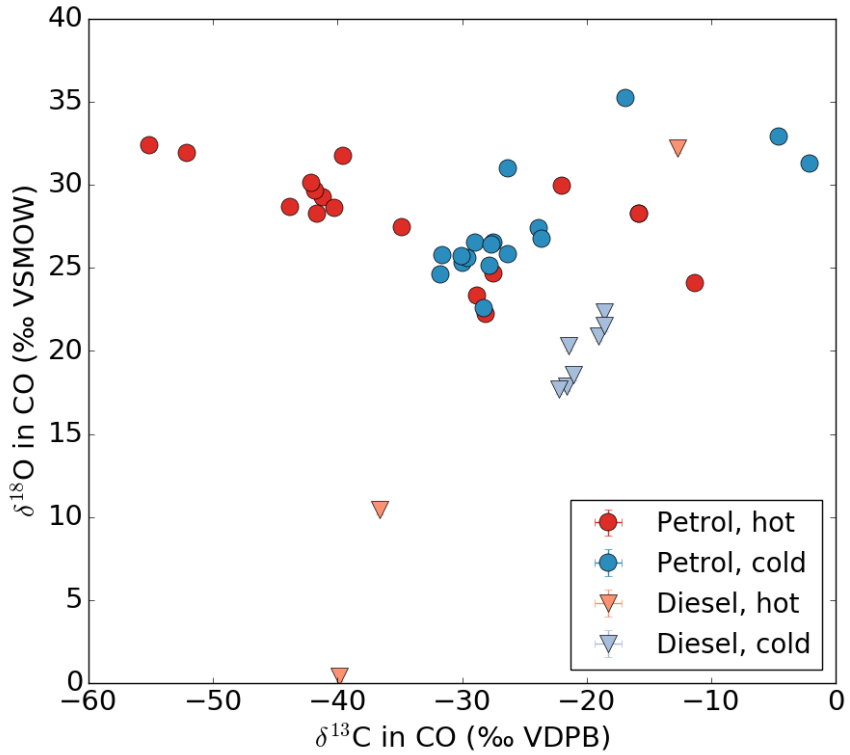

Figure 2: The results for the δ^{18}O values in CO plotted against the δ^{13}C values in CO from the cars sampled under idling conditions. Dark-coloured circles indicate petrol cars and light-coloured triangles diesel cars. Hot and cold cars are shown in red and blue respectively.

fuel type, mileage and the year of manufacture were noted. Arriving cars were labelled as hot and departing cars as cold. The specifics for which the largest differences were found, are whether the car was hot or cold and the fuel type. Therefore, these groups are distinguished in the figures.

The isotopic composition of CO in car exhaust is shown in Figure 2. It is clear that there is considerable spread in the results. For δ^{18}O this spread is dominated by a few points: most of the results are in the 20 to 35 ‰ range (except for diesel). For δ^{13}C the spread is more uniform and covers a range from -60 to 0 ‰ range. The two isotopic components show no clear correlation.

From this figure it is clear that there are distinct groups in the data. The most well-defined group is that of cold diesel cars, which are all centred around δ^{13}C = -20 ‰ and δ^{18}O = +20 ‰. The second group contains most cold petrol cars and is centred around a δ^{13}C = -30 ‰ and δ^{18}O = +25 ‰. These values are similar to what is reported in literature. The hot cars and the remainder of the cold petrol cars dominate the spread. Overall hot petrol cars emit CO depleted in δ^{13}C and slightly enriched in δ^{18}O compared to cold petrol cars, but enrichment in δ^{13}C and depletion in δ^{18}O is also present. Judging from this figure alone, it could be a considerable challenge to determine a well-defined atmospheric signature of traffic from individual car measurements.

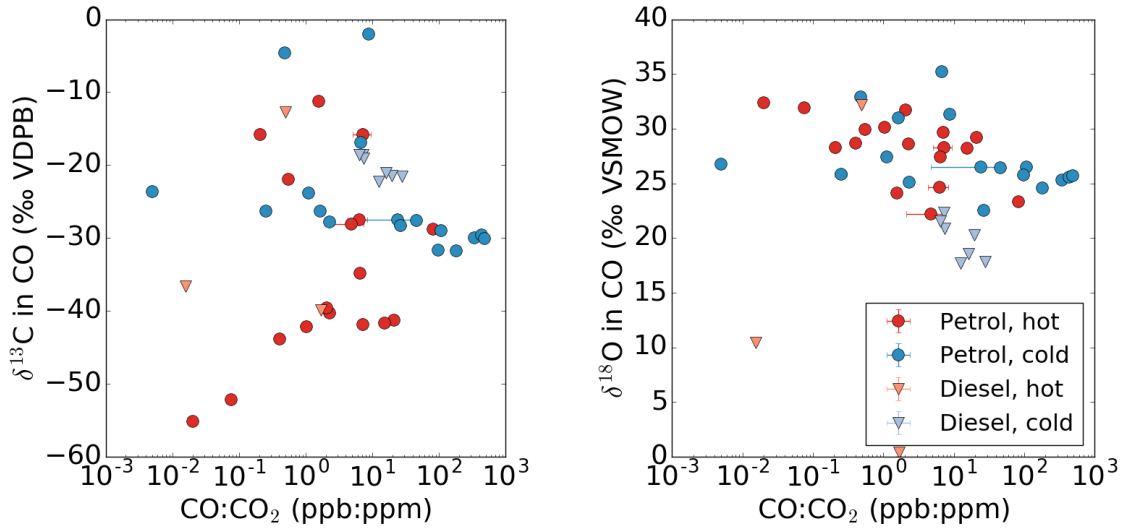

(a) δ^{13}C versus CO:CO$_2$.

(b) δ^{18}O versus CO:CO$_2$.

Figure 3: The δ^{13}C (a) and δ^{18}O (b) values of CO plotted against the CO:CO$_2$ ratio for the samples taken from idling cars. The CO:CO$_2$ ratio is plotted logarithmically.

δ^{13}C and δ^{18}O values are plotted against the CO:CO$_2$ ratio in Figures 3a and 3b respectively. The CO:CO$_2$ data are found in a range that spans roughly 5 orders of magnitude. Between 10^{-1} and 10^{2} ppb:ppm the distribution is quite uniform.

Though at first glance there is no clear correlation between CO:CO$_2$ and δ^{13}C , it is obvious that the highest emitters, mostly cold cars, emit quite CO with a relatively constant isotopic composition. For δ^{13}C and δ^{18}O this value is -30 ‰ and +25 ‰ respectively: the same composition around which the cold petrol cars were grouped in Figure 2. When only the cold petrol cars are considered, there does seem to be a correlation between CO:CO$_2$ and δ^{13}C . Lower concentrations are associated with more depleted δ^{13}C values. If a TWC removes ^{12}C^{16}O at a different rate than ^{13}C^{16}O, and if TWC efficiency is the only factor affecting the CO:CO$_2$ ratio, then it is indeed expected that δ^{13}C and CO:CO$_2$ are correlated.

To study this depletion, I determined the fractionation constant ϵ, which is defined as:

$$\epsilon = \frac{k'}{k} - 1. \tag{3}$$

k and k' are the reaction coefficients of some compound (here ^{12}C^{16}O) and its isotopologue (here ^{13}C^{16}O) respectively. Therefore, ϵ gives the difference in removal rates of the two isotopes, similar to how δ gives the difference in concentrations. It can be shown that, for removal by one source, the following equation holds:

$$\ln(1 + \delta^{13}\mathrm{C}) = \epsilon \cdot \ln(\frac{(\mathrm{CO} : \mathrm{CO_2})_{\mathrm{meas}}}{(\mathrm{CO} : \mathrm{CO_2})_{\mathrm{prod}}}) + \text{constant}. \tag{4}$$

Here (CO:CO$_2$)$_{\mathrm{meas}}$ is the CO:CO$_2$ ratio that is measured and (CO:CO$_2$)$_{\mathrm{prod}}$ the ratio that the car initially produces. The equation holds under the assumption that CO$_{2,\mathrm{meas}} \approx$

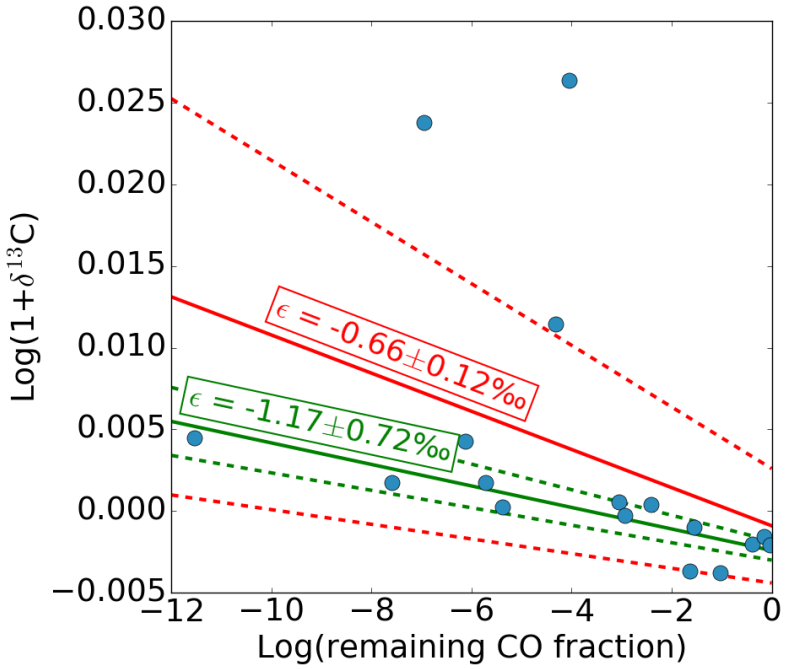

Figure 4: A Rayleigh plot for δ^{13}C and CO:CO_2, only including the cold petrol cars. Two fits are given: one including the three outliers (red) and one only including points close to the fit (green). Dashed lines outline the 68% confidence intervals of the fits.

$CO_{2,\mathrm{prod}}$, which, for a car, is indeed the case. If the logarithm of 1+ δ^{13}C (relative to the source value) is plotted against the logarithm of the remaining CO:CO_2 fraction, a linear relation is expected. The slope of the best fit then gives ϵ. Only cold petrol cars are included, since it is unlikely that diesel and petrol cars use the same removal process. The resulting plot, along with a fit to the data, is shown in Figure 4. For this plot it is necessary to assume that each car engine produces the same CO:CO_2 ratio. To ensure the remaining fraction is smaller than 1 for all samples (i.e. no CO is produced after the air leaves the engine), this initial ratio is chosen as of 500 ppb CO per ppm CO_2. Varying this value between 100 and 800 ppb:ppm has no significant influence on ϵ. In addition the δ^{13}C value of the source is chosen as -28 ‰, the average value for carbon in petrol. Again, changing this by several per mil has no influence on the resulting fractionation.

Under these assumptions a value for ϵ of -1.2 ± 0.72 ‰ is found. However, 3 cold petrol samples clearly behave differently from the rest. These are also outliers in Figure 2. Excluding these samples leads to an ϵ of -0.66 ± 0.12 ‰. Both fits are shown in Figure 4. The only two other reported values of this parameter are -2.7 ± 0.6 ‰ (Popa et al., 2014) and -2.6 ‰ (Tsunogai et al., 2003). Though of the same sign, the fractionation found here is significantly smaller. Since the spread in the δ^{13}C values of the selected samples is small, the relation found here could be coincidental. Moreover, if this were indeed the correct value for ϵ, it is unclear where the large spread in the isotopic composition of CO in hot cars comes from.

In the plot of δ^{18}O versus CO:CO_2 (Figure 3b) the data is distributed in a uniform cloud, with a few outliers. There is no significant correlation between δ^{18}O and CO:CO_2.

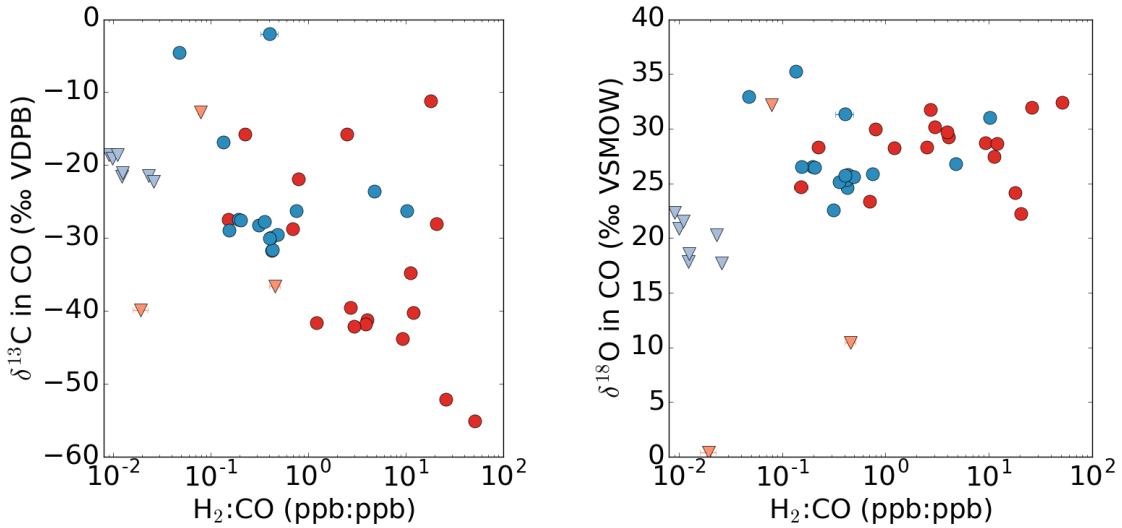

(a) δ^{13}C versus H_2:CO.

(b) δ^{18}O versus H_2:CO.

Figure 5: The δ^{13}C (left) and δ^{18}O (right) values of CO plotted against the H_2:CO ratio for the samples taken from idling cars. The H_2:CO axis is logarithmic.

The cold diesel cars again form a well-defined group around a CO:CO_2 ratio of 10 ppb:ppm. These emissions are not insignificant compared to the values reported for petrol cars in literature. However, the highest emitting petrol cars found here emit several orders of magnitude more CO than the diesel cars.

δ^{13}C and δ^{18}O values of CO are plotted against the H_2:CO ratio in Figures 5a and 5b respectively. The spread in H_2:CO, as in all other parameters, is large. It is striking that the same group of cold petrol cars found as a group in other figures is centred around a H_2:CO ratio of 0.5 ppb:ppb: the same value that is reported in the literature. The cold diesel cars all show low H_2:CO values.

There seems to be a correlation between H_2:CO and δ^{13}C . More specifically, there seems to be a lower cut-off line below which no combination of H_2:CO and δ^{13}C is found: no depleted δ^{13}C values are found when H_2:CO is low. No such correlation is found between δ^{18}O and H_2:CO.

In Figure 6 the CH_4:CO_2 ratio is plotted against the CO:CO_2 ratio. It can be seen that, especially for high emitters, there is a strong correlation between CO and CH_4 emission factors. At lower emission ratios the spread increases.

On several occasions a car was sampled twice, either closely after one another or on different days. Generally, the variation between these two samples was no smaller than the variation between any two different cars. This shows that the internal state of the car (engine, TWC) has a significant influence on the exhaust composition and that this internal state shows strong and quick temporal variations.

In most figures hot and cold cars seem to form two different clusters. To test whether these groups deviate from one another significantly a Welch's t-test was performed. A Welch's t-test works from the null hypothesis that two different groups of samples have equal means. It is an extension on the simpler Student's t-test and it is intended for the

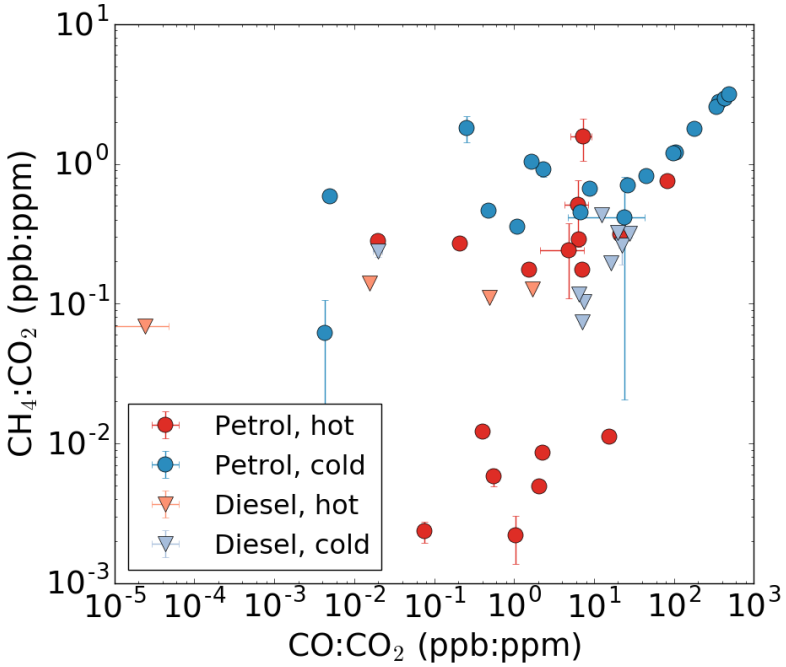

Figure 6: Results for the CH_4:CO_2 ratio plotted against the CO:CO_2 ratio, from the cars sampled under idling conditions. Both axes are logarithmic.

comparison of two independent sample groups of different sizes and different variances. Only petrol cars are considered, because petrol and diesel cars are not necessarily expected to behave similarly and the diesel sample size is too small to make a separate t-test meaningful. The parameters were tested on a significance level of 5%. A p-value smaller than 5% means that the null hypothesis that the two groups are similar is rejected with 95% confidence. The result for each parameter is shown in Table 5.

Parameter	Mean cold	Mean hot	p-value (%)
δ^{13}C (‰)	-25.5 ± 8.5	-34.2 ± 12.4	1.5
δ^{18}O (‰)	28.2 ± 2.9	27.3 ± 2.9	44.6
H_2:CO (ppb ppb^{-1})	1.2 ± 2.4	10.6 ± 13.2	1.6
CO:CO_2 (ppb ppm^{-1})	111.8 ± 160.6	9.9 ± 19.6	1.5
CH_4:CO_2 (ppb ppm^{-1}	1.3 ± 0.9	0.3 ± 0.4	0.05

Table 5: The mean and standard error of the mean (SEM) of the parameters for petrol cars, split between hot and cold cars. The last column gives the results from Welch's t-test. For $p < 5\%$ the hypothesis that the two groups have equal means is rejected at the 95% (3-σ) confidence limit.

To varying degrees hot and cold cars have significantly different means for δ^{13}C ,

H_2:CO, CO:CO_2 and CH_4:CO_2. For $\delta^{18}O$ the distinction is not significant, possibly because of the small spread in the $\delta^{18}O$ results. This makes it clear that hot and cold cars exhibit different behaviour for most of the emission parameters.

Besides the distinction between hot/cold and diesel/petrol, correlations between emission parameters and mileage, year of manufacture, engine type or car type were investigated. However, no clear correlation was found for any of these parameters. The corresponding figures are given in Appendix E. This does not exclude any influence of these parameters on car emissions, but, because of the large spread in the data, a bigger sample size is probably needed to find a signal.

4.2 Testbench measurements

For the measurements on the testbench three petrol cars were used, the characteristics of which are given in Table 6.

Car number	Car type	Manufacture year	Mileage (x 1000 km)
1	Smart Forfour	2007	103
2	Citroën Berlingo	2006	224
3	Ford Focus	2016	1

Table 6: The vehicle characteristics of the cars used for the test bench measurements.

The cars were sampled under similar driving cycles. Because of the large spread found in the data up to this point, each driving condition was sampled several times. First the car was measured while idling, for comparison with previous results. Then the car was driven at 50 km/h. To give an indication of what happens to emissions while the car is heating up, 6 to 8 samples, over a period of 15-20 minutes, were taken at this speed. Then the speed was increased to first 90 and then 120 km/h. Next the car was accelerated from 0 to 50 km/h in $\sim$ 30 seconds. Because of the switching of gears, constant acceleration was only maintained from $\sim$ 15 to 50 km/h (in second gear), so that this was the period in which samples were taken. Finally, some more idling samples were taken.

The Ford Focus had several modern safety measures, which did not allow any speeds above 25 km/h under conditions present on the test bench (e.g. only front wheels turning). It is therefore unlikely that during any part of the sampling, except during the first idling samples, the car was actually cold.

The results for the three cars are displayed in Figure 7. The spread found in the isotope results for idling cars (see Figure 2) is present in each of the individual cars. In some cases jumps of several tens of per mil between two subsequent samples are found. In general CO emissions of these cars are quite low (CO:CO_2 $<$ 10 ppb:ppm). The exception are the first idling sample for both car 1 and 2, which had CO:CO_2 ratios of 393 ppb:ppm and 44 ppb:ppm respectively. The isotopic values that correspond to these high CO:CO_2 ratios are close to -30 ‰ and +25 ‰ for $\delta^{18}O$ and $\delta^{13}C$ respectively and the H_2:CO ratio is between 0.1 and 0.6 ppb:ppb, similar to what was found earlier for high emitters. Except for the same two samples, CH_4:CO_2 emissions were also low.

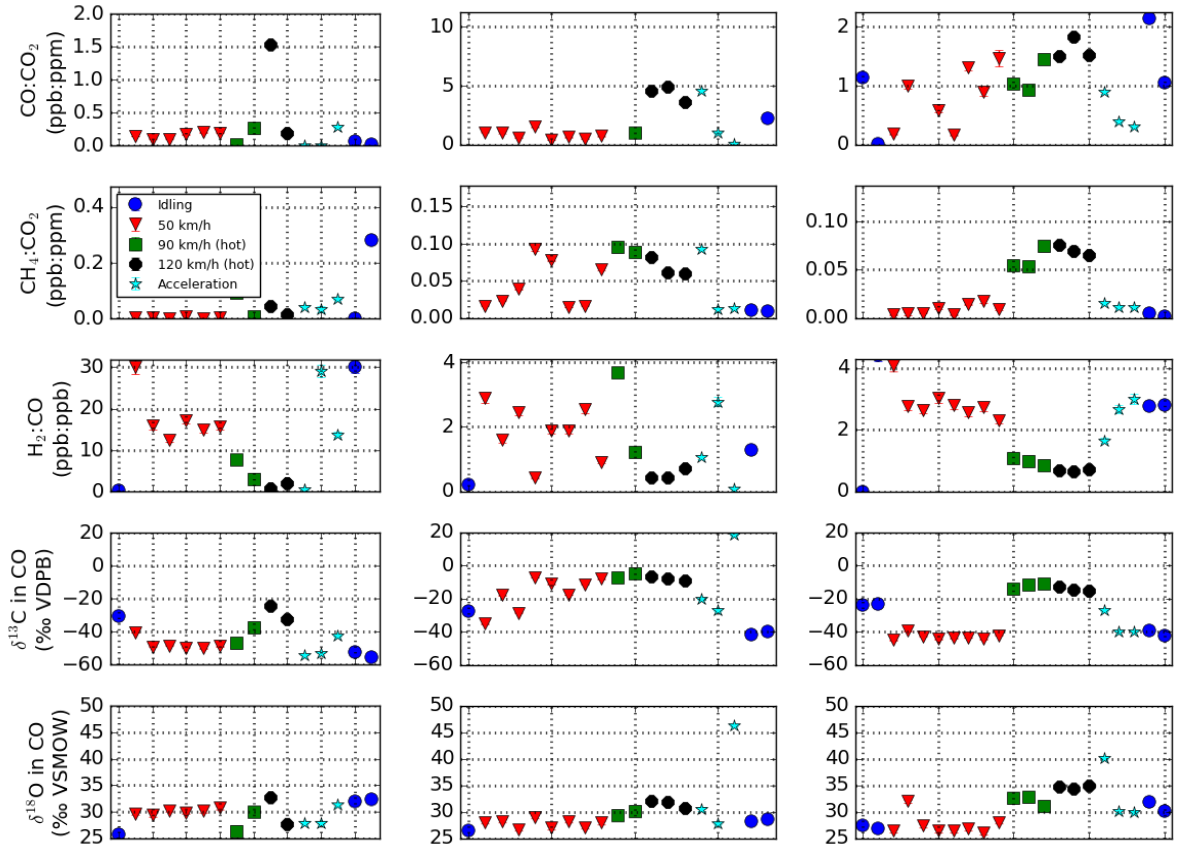

(a) Car 1: the Smart Forfour (2007). **(b)** Car 2: the Citroën Berlingo (2007). **(c)** Car 3: the Ford Focus (2016).

Figure 7: The testbench results, where each car is plotted in a separate figure. Results are plotted in the chronological order in which the samples were taken. Each driving condition is indicated by a different shape and colour, the meaning of which is given in the legend.

It is not possible to deduce a systematic pattern, or the influence of driving conditions from these results. The results are, compared to the strong temporal variations found in idling cars, more consistent. Looking at any one car, correlations between driving conditions and emissions could be established. However, most of these correlations don't hold for the other cars. Higher driving speeds do correspond to elevated CO and CH_4 emissions, though not for every sample. For car 3 changes in isotopic composition and gas ratios are very sudden, suggesting a strong influence of the driving speed. However, for car 1 and 2 changes are more gradual, suggesting there is a memory effect in the emissions. Acceleration is expected to push a car's engine away from equilibrium, leading to sub-optimal performance and higher emissions. This is not seen in the results. It could be that the acceleration used in this test was too weak, or that modern cars have sufficient buffering capacity to remain largely unaffected by sudden changes in driving conditions.

Previously we found indications for a connection between H_2:CO and δ^{13}C . For car 1 and 3 higher H_2:CO ratios indeed seem to correspond to more depleted δ^{13}C values. For car 2 no such behaviour is observed. It is worth noting that the spread in H_2:CO for car 2 and 3 is quite small compared to that measured in idling cars. In the end, there is no one-to-one relation between H_2:CO and δ^{13}C . δ^{13}C and δ^{18}O are slightly positively correlated, especially when strong variations occur. δ^{18}O variations are again relatively small, in the same range as what was seen for the idling results.

4.3 Revving results

In this section results from the revving samples are discussed. This approach was used in at least one other study (Kato et al., 1999) and is used to induce some additional engine load. Four cars were measured, of which 2 were petrol and 2 were diesel cars. One of these, the Citroën Berlingo, was also measured on the testbench. I sampled each of the cars while a driver pressed the accelerator to varying degrees. In general a few samples were taken under idling conditions ($\sim$ 700-800 rpm), under a slightly elevated engine load ($\sim$ 1200-1300 rpm) and under a more strongly elevated engine load ($\sim$ 1800-2000 rpm). Before starting the sampling, each car had been standing still long enough that they very likely started out cold. It is unlikely that any of the cars heated up completely, because the engine load of pressing the accelerator without coupling is low.

The results showed large variations, which could be both sudden or gradual, similar to the testbench measurements. However, there were no clear patterns in the data and each car reacted differently to variations in the engine load. Since these results do not provide additional insight to the testbench measurements and since they were generally more unstable, they are not discussed in as much detail. The important characteristics of the revving data can be deduced from the aggregated results, which are presented in section 4.4.

4.4 All results combined

Up to this point, it is not completely clear how the idling, the testbench and the revving results fit together. For this purpose, the plots that showed the most interesting characteristics in section 4.1, are again given here, with the revving and testbench measurements added. Some testbench and revving samples are actually idling samples and were already

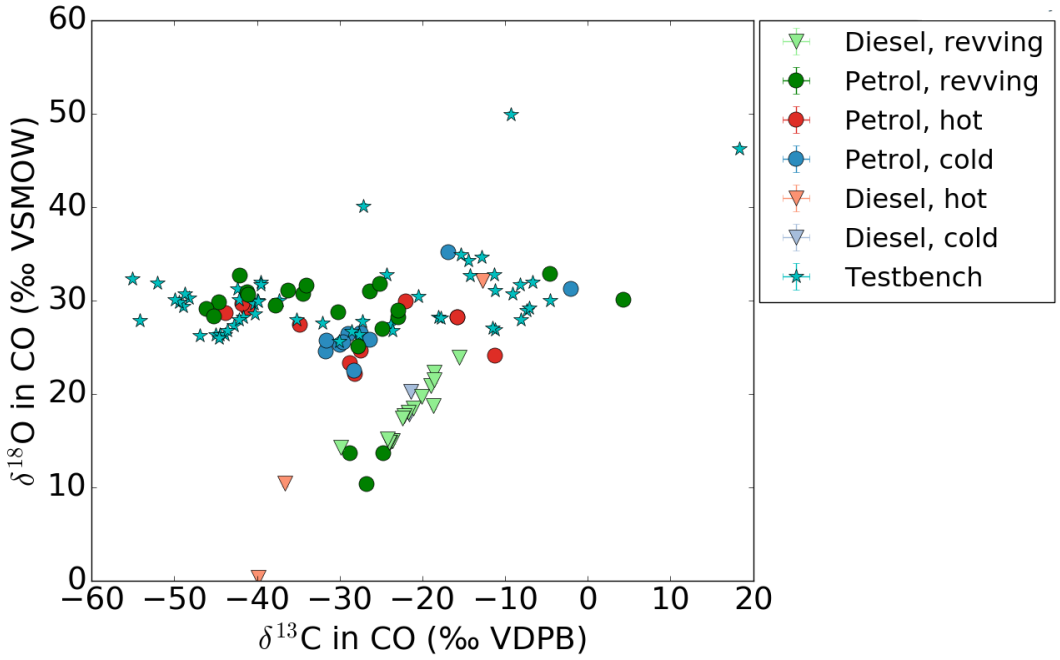

Figure 8: δ^{18}O plotted against δ^{13}C with all samples (idling, testbench and revving) included. The testbench measurements are indicated by cyan stars. The revving samples are indicated by dark green circles and light green triangles for petrol and diesel respectively. Idling samples are indicated the same as in Figure 2.

included in section 4.1, so that there is some overlap. These idling samples are labelled here as 'Testbench' and 'Revving' respectively, and not as 'Idling', to keep the distinction between the different approaches transparent. For the revving samples, a distinction between diesel and petrol cars is made. All cars tested on the testbench drove on petrol. In both cases no distinction between hot and cold cars is made, since most samples likely fall somewhere in between the two extremes. The results are shown in Figures 8 (δ^{18}O against δ^{13}C), 9 (δ^{13}C against H_2:CO) and 10 (CH_4:CO_2 against CO:CO_2).

The most important characteristics found in section 4.1 are summarized below, with an interpretation of how the additional data confirms or changes them.

1) **(Cold) diesel cars form a distinct group for all parameters.**

   All added diesel samples come from the revving measurements. It is clear that most of these fall into the previously defined group, with δ^{13}C $\approx$ 20 ‰, δ^{18}O $\approx$ -20 ‰, a low ($< 10^{-1}$ ppb:ppb) H_2:CO ratio, a CO:CO_2 ratio of 10 ppb:ppm and a CH_4:CO_2 ratio of 10^{-1} ppb:ppm. Only a few samples do not conform to this group. The additional points also reveal that there might be a positive correlation between δ^{18}O and δ^{13}C for this group of samples. Even the diesel samples that do not follow the other characteristics of this group, fall approximately along this line. The correlation between CO:CO_2 and CH_4:CO_2, found for the highest emitters, can be extrapolated to this diesel group (Figure 10), even though their absolute emissions do not characterize them as the highest emitters.

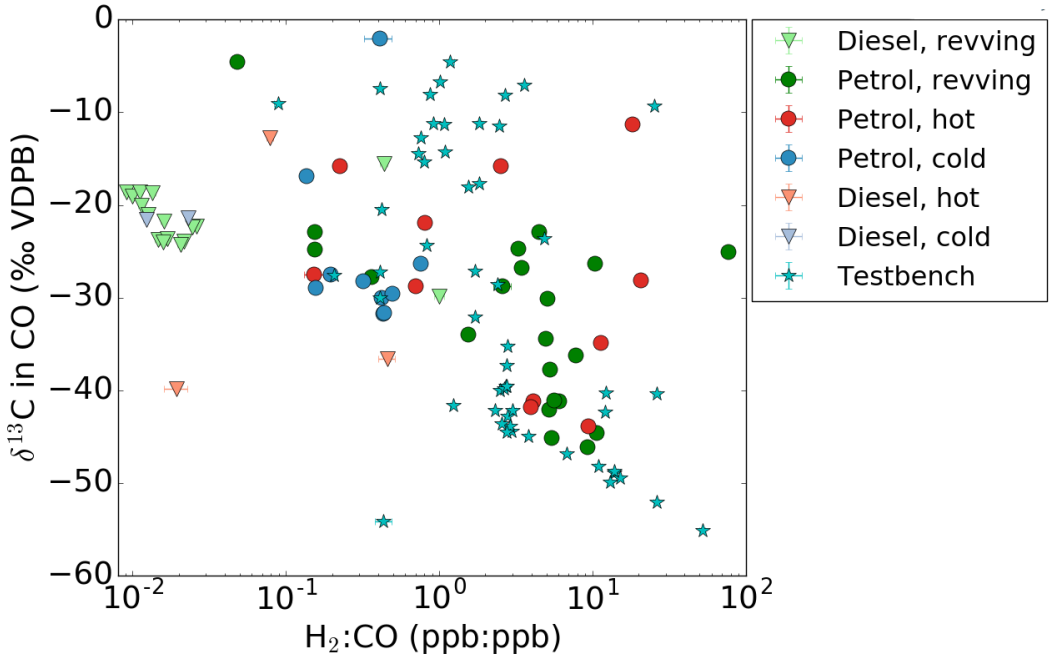

Figure 9: δ^{13}C plotted against H_2:CO with all samples (idling, testbench and revving) included. H_2:CO is plotted logarithmically.

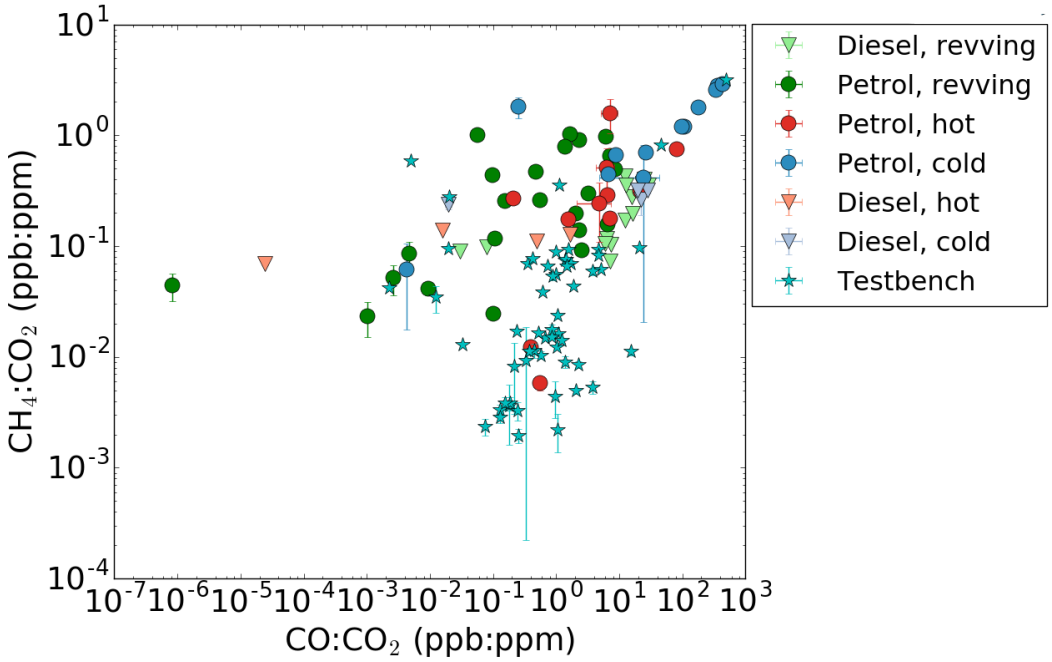

Figure 10: CO:CO_2 plotted against CH_4:CO_2 with all samples (idling, testbench and revving) included. Both axes are logarithmic.

2) **H_2:CO and $\delta^{13}C$ show a weak negative correlation. Moreover, there is a cut-off line, below which no samples are found.**

The overall correlation is weaker than for the idling samples alone: the additional samples mostly add to the spread. However, all spread is still located above the cut-off line, except for 1 sample. In a sample size of 126 this can be considered an anomaly. The cut-off line itself becomes more well-defined by the new samples.

3) **The samples with the highest CO:CO_2 ratios, mostly cold petrol cars, all show a similar isotopic composition for CO with $\delta^{13}C \approx$ -30 ‰ and $\delta^{18}O \approx +25$ ‰ as well as a H_2:CO ratio of 0.1-0.6 ppb:ppb.**

This finding still holds, but no additional high emitters were added, so that no additional confirmation was found either. The additional samples, especially those from the testbench mostly increase the spread in both the isotopic composition of CO and H_2:CO.

4) **There is a positive correlation between CH_4:CO_2 and CO:CO_2, especially for high emitters.**

No more high emitters were added. However, the revving results reveal that the correlation can be extrapolated to the diesel samples.

4.5 The isotopic composition of CO_2

In addition to the isotopic composition of CO, the isotopic composition of CO_2 was measured for a selection of 34 samples. Figure 11 shows the isotopic signature of CO_2 for the samples measured. The spread in $\delta^{13}C$ is much smaller than what was found for CO. Moreover, most of the spread comes from spread between cars. Therefore, the $\delta^{13}C$ in CO_2 indeed seems to reflect that of fuel, which, for these samples, covers a range of -29.5 to -27.5 ‰ . Since oil from different regions has different $\delta^{13}C$ values, some variation between cars is expected. For $\delta^{13}C$ in CO_2, no difference between petrol and diesel cars is found.

The $\delta^{18}O$ values cover a larger range, from 20 to 35 ‰, similar to what was found for $\delta^{18}O$ in CO (e.g. Figure 8). However, as can be seen in Figure 12, the results are not correlated. $\delta^{18}O$ values of CO_2 from diesel cars are a lot more constant, centred around $\delta^{18}O = +23$ ‰. This is very different from the $\delta^{18}O$ of CO (Figure 12), which, for these samples, shows more spread than the $\delta^{18}O$ of petrol samples.

4.6 Parking garage measurements

To complement the individual car exhaust measurements, I took a number of samples in and near different parking garages. The samples were taken over a number of days. I took the samples either in the early morning or in the late afternoon: the two times at which car activity is expected to be at its highest. These measurements are expected to give a measure of the isotopic composition of CO averaged over a larger number of cars.

The $\delta^{13}C$ values are plotted versus the CO concentration ([CO]) in Figure 13a. The CO concentration is in some cases indeed significantly elevated and higher CO concentrations seem to correspond with more depleted $\delta^{13}C$ values. To derive a source signature, I made

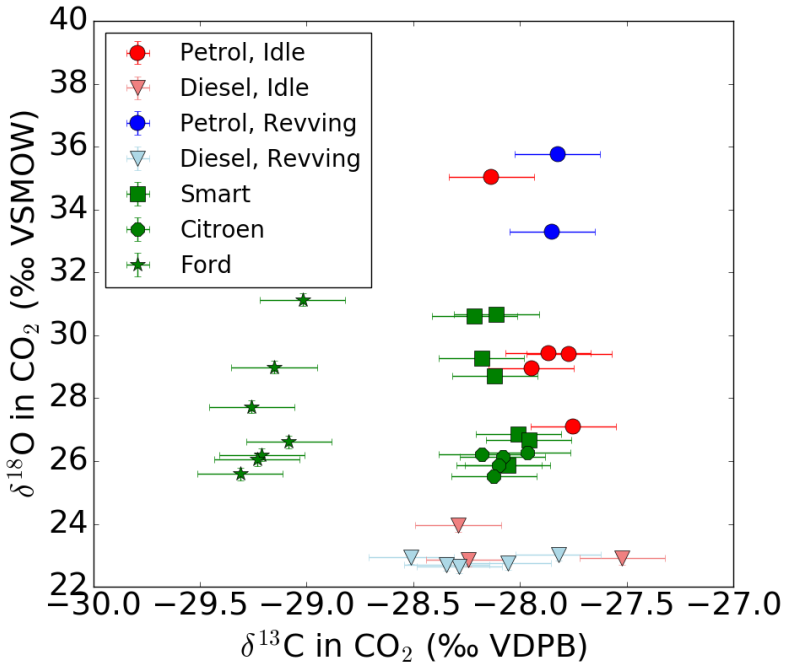

Figure 11: The results from the CO_2 isotope measurements of a select set of samples. Idling samples are indicated in red and revving samples in blue. Diesel samples are indicated by light triangles and petrol samples by dark circles. Testbench measurements are indicated in green and the different cars are distinguished by different symbols.

a Keeling plot, in which the reciprocal of [CO] is the independent variable. We assume all additional CO above the (constant) background level is emitted by cars. Then the $\delta^{13}C$ value that is measured is given by:

$$\delta^{13}C_{\text{measured}}[CO]_{\text{measured}} = \delta^{13}C_{\text{background}}[CO]_{\text{background}} + \delta^{13}C_{\text{cars}}[CO]_{\text{cars}}, \tag{5}$$

or, in a different form:

$$\delta^{13}C_{\text{measured}} = (\delta^{13}C_{\text{background}} - \delta^{13}C_{\text{cars}})\frac{[CO]_{\text{background}}}{[CO]_{\text{measured}}} + \delta^{13}C_{\text{cars}}, \tag{6}$$

where we used $[CO]_{\text{measured}} = [CO]_{\text{background}} + [CO]_{\text{cars}}$. Therefore, a Keeling plot for contamination by a single source should show a straight line, where the intercept with y-axis gives the source value. For $\delta^{18}O$ and for H_2:CO the same equations hold. The derivation for H_2:CO is given in Appendix D.

Figure 13b shows the result for $\delta^{13}C$. A least-squares, linear fit to the data gives a source value for $\delta^{13}C$ of -29.5 ± 0.4 ‰.

I made similar plots for both $\delta^{18}O$ and H_2:CO, shown in Figure 14 and 15 respectively. Though the spread seems smaller in these plots, the relative range on the y-axis is also larger. The accuracy of the source values is similar for all parameters. For $\delta^{18}O$ a source value of 25.9 ± 0.4 ‰ is found and for H_2:CO a value of 0.46 ± 0.06 ppb:ppb. Since the samples were taken on different days, background levels were not constant, so that some contamination by other sources might be present. Therefore, it is interesting that this

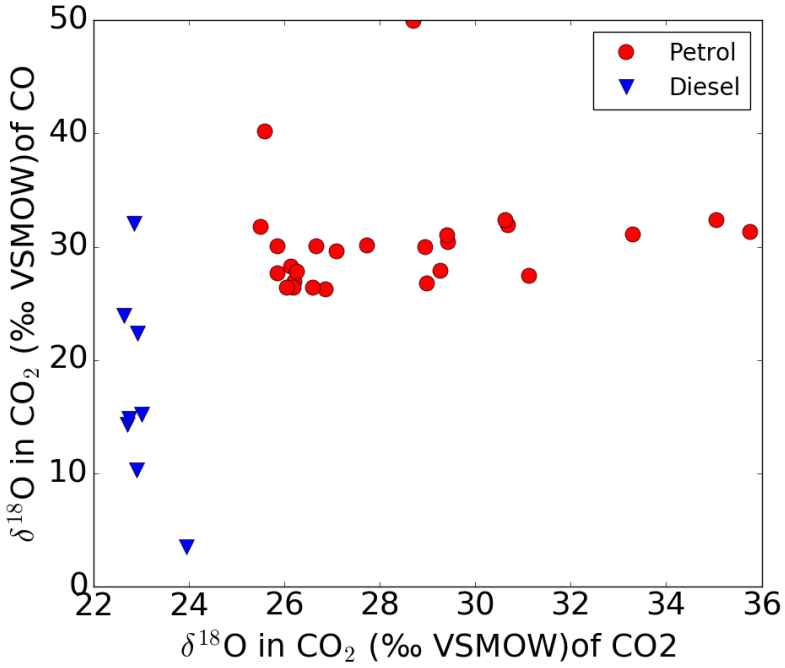

Figure 12: The δ^{18}O values of CO plotted against the δ^{18}O values of CO_2, for the samples that were measured for the isotopic composition of CO_2. Red circles indicate petrol cars and blue triangles indicate diesel cars.

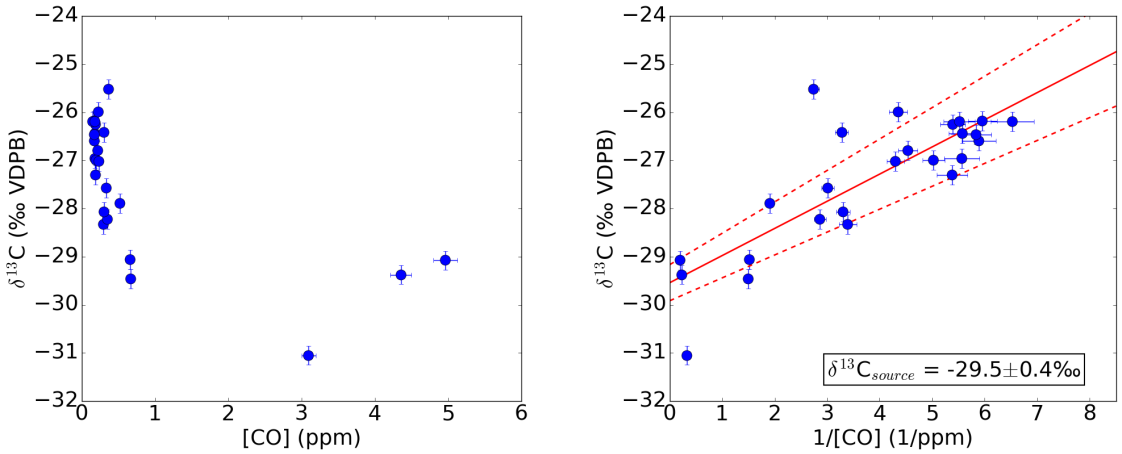

(a) δ^{13}C versus [CO]. **(b)** δ^{13}C versus 1/[CO].

Figure 13: The results for δ^{13}C and CO in the parking garage measurements. Both a plot of δ^{13}C versus [CO] (a) and the corresponding Keeling plot (b) are given. In the Keeling plot, a least-squares, linear fit is given by the solid line, while the dashed lines outline the 68% confidence interval of the fit.

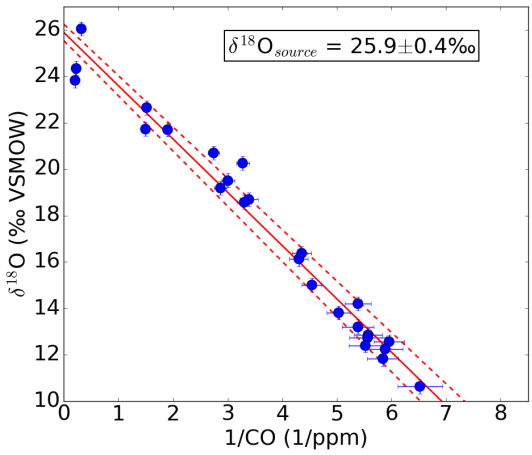

Figure 14: A Keeling plot of δ^{18}O versus 1/[CO]. A least-squares, linear fit is given by the solid line, while the dashed lines outline the 68% confidence interval of the fit.

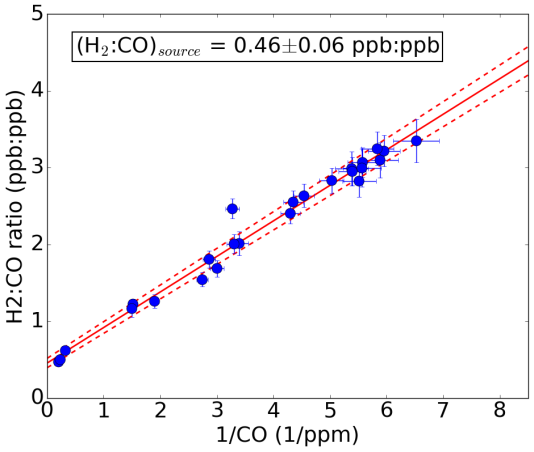

Figure 15: A Keeling plot of H2:CO versus 1/[CO]. A least-squares, linear fit is given by the solid line, while the dashed lines outline the 68% confidence interval of the fit.

simple approach leads to reasonable results, which are in good agreement with literature values. It shows that the large spread found when sampling individual cars in some way evens out in the atmosphere.

Interestingly, a Keeling plot for the CO:CO_2 ratio shows no linear relation. A likely explanation is that even with strong pollution the CO_2 increase is only $25-50\%$ of the background level, while CO and H_2 can be elevated by over 1000%.

4.7 Order in chaos

Throughout this study huge spread in the isotopic composition of CO from cars was found. However, when measuring in a parking garage, a very basic approach reproduced literature values remarkably well. The isotopic composition of individual cars is centred approximately around these literature values, but it is unlikely that the spread would even out so well in a parking garage, since the pollution in a garage is the combination of only a relatively small number of cars.

A different explanation could be that the isotopic signature of traffic is dominated by a few moments of high emissions. It was previously seen that the highest emitters have an isotopic composition close to what was found in section 4.4. To check this explanation for δ^{13}C , Figure 16 shows a histogram of all the data in this study for δ^{13}C . However, a histogram alone would not tell much, because the distribution visible is biased by the types of samples taken in this study. The sample distribution was not chosen to represent any driving cycle, so that it is unlikely that it actually does. For this reason the mean CO:CO_2 ratio of the samples in each bin is also plotted.

Given this combination of data, it becomes clear why the isotopic signature of CO from traffic is well-defined. The samples centred around this signature are those with concentrations over one order of magnitude larger than the rest. The sample distribution

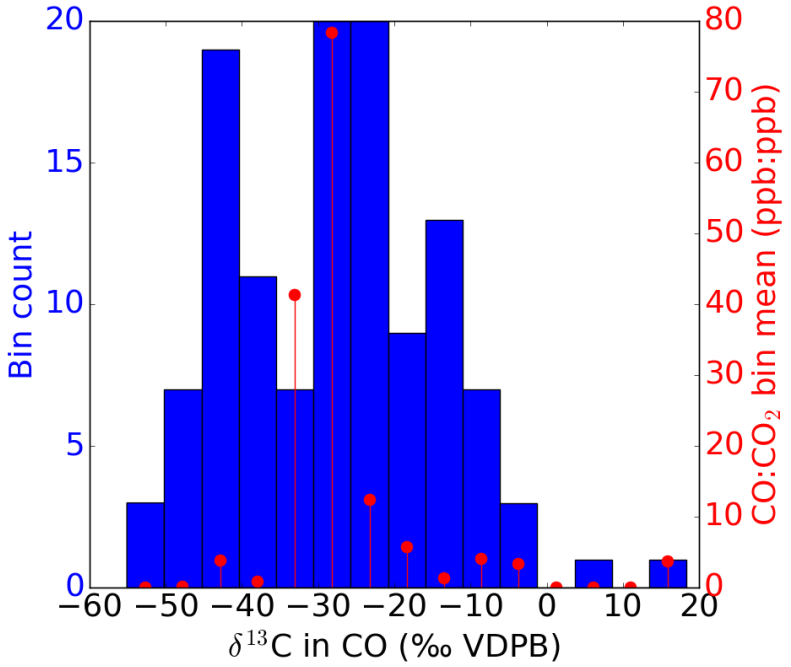

Figure 16: A histogram of all δ^{13}C data collected in this study. Blue (left axis): The number of samples in each bin. Red (right axis): The mean CO:CO_2 of the samples in the bin.

itself may change strongly when this study is repeated with an emphasis on different driving conditions, but the distribution of CO:CO_2 means is so pronounced that it is likely more robust. Similar plots for H_2:CO and δ^{18}O are given in Figure 17. These show the same behaviour, though for H_2:CO the distribution is more skewed towards zero.

To determine what this behaviour means for the atmospheric signature of traffic, I computed what the final traffic signature would be, if all the flasks were combined. For the δ-values this is computed using: $\delta_{final} = \frac{\sum_{i=1}^{N}[CO]_i\delta_i}{\sum_{i=1}^{N}[CO]_i}$. For H_2:CO the result is given by $\frac{\sum_{i=1}^{N}[H_2]_i}{\sum_{i=1}^{N}[CO]_i}$. The weighted means are given in Table 7.

The isotopic composition of CO found here is remarkably close to that found in the parking garage measurements, especially for the idling data. Moreover, the standard errors of the mean (SEM) are small, compared to the overall spread in the data. For H_2:CO the results even out less well. Different from the isotopic composition, samples with low CO concentrations can still contribute significantly to the final H_2:CO ratio, if they have a high H_2 concentration.

To visualize the influence of the samples with high CO:CO_2 values, Figure 18 shows what happens to the mean δ^{13}C and δ^{18}O if the top x samples are dropped. It is clear that if the 5 highest emitters are dropped, both δ values are strongly affected. This behaviour is explained when looking at the remaining CO:CO_2 fraction, also given in Figure 18.

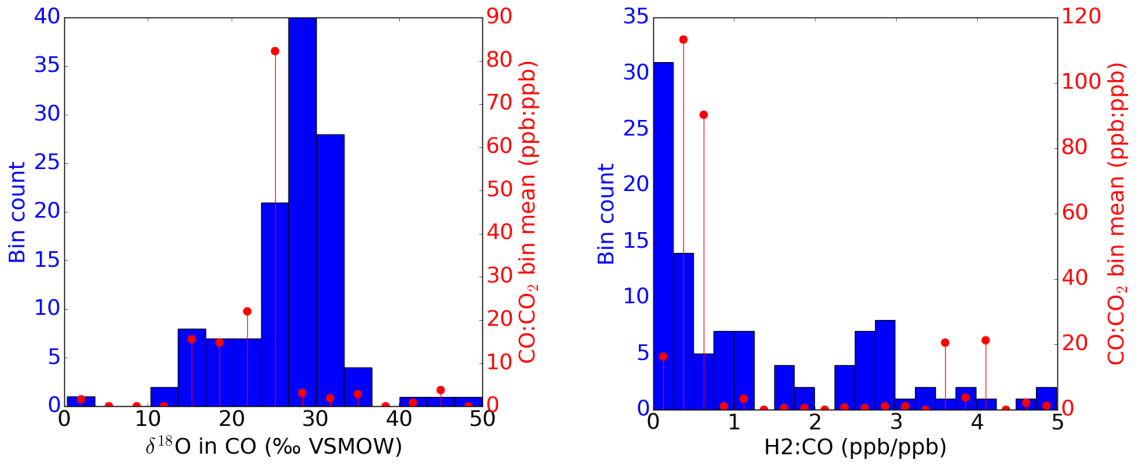

(a) The results for δ^{18}O .

(b) The results for H_2:CO.

Figure 17: A histogram of all δ^{18}O and H_2:CO data collected in this study. Blue (left axis): The number of samples in each bin. Red (right axis): The mean CO:CO_2 of the samples in the bin.

Parameter	Overall	Idling
δ^{13}C (‰)	-28.7 ± 0.5	-29.6 ± 0.5
δ^{18}O (‰)	24.8 ± 0.3	25.3 ± 0.3
H_2:CO (ppb:ppb)	0.71 ± 0.31	0.62 ± 0.29

Table 7: The means and standard errors of the mean (SEM) computed from all data in this study, for the parameters found to have a well-defined traffic signature. For the δ values the weighted mean was used, with the CO:CO_2 ratio as the weight. For H_2:CO the sum of the H_2 concentrations was divided by the sum of the CO concentrations. This was done both for the idling data as well as for the overall data.

The 5 highest emitters make up 70% of the total sum of CO:CO_2 ratios of all samples, so that they dominate the weighted mean calculations.

Figure 18 shows that dropping the highest emitters, leads to enrichment in both δ^{13}C and δ^{18}O of CO in the weighted mean of the remaining samples, for the top $\sim$ 60 samples. The samples with the lowest concentrations are the ones most depleted in δ^{13}C .

The weighted mean calculations were also done for the distinct groups identified in the data: cold petrol cars and cold diesel cars. The overall results for the isotopic composition of CO as well as for each of the gas ratios, are summarized in Table 8. This confirms the findings up to this point. The values for δ^{13}C , δ^{18}O and H_2:CO found in the parking garage are best represented by the cold petrol cars. Including all samples shifts these values somewhat, but especially the isotopic values do not change much. The cold diesel cars indeed form a distinct group, with a distinct isotopic signature, as well as with a very low H_2:CO ratio. The CO emissions of cold diesel cars are actually quite significant compared to the overall results, though the few hot diesel cars sampled showed that these

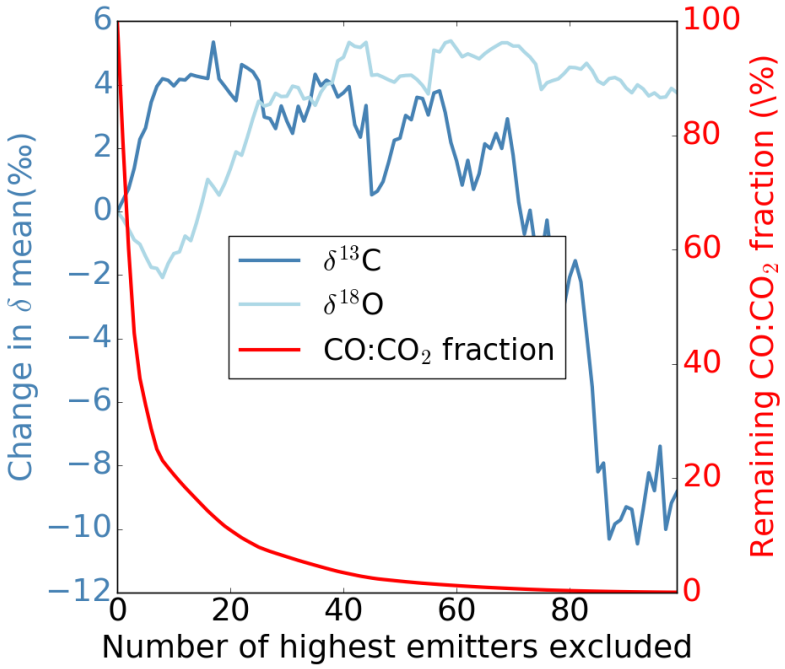

Figure 18: The change in the δ^{13}C (dark blue) and δ^{18}O (light blue) mean (left axis) and the fraction of the sum of CO:CO_2 in the samples remaining (red, right axis) plotted against the number of highest emitters that are excluded from the calculations.

emissions sharply drop off when the car heats up. It is interesting that the differences between the groups for CO:CO_2 are very similar to those for CH_4:CO_2, again confirming that there is a connection between these two gas ratios.

5 Discussion

5.1 CO isotopes

As is mentioned in section 1.4, research into CO isotopes from individual car measurements up to this point is rare and sparsely spread through time. With the knowledge obtained in this paper it is interesting to review previous findings. Kato et al. (1999) found a well-defined isotopic signature in their measurements: a δ^{13}C -29.9 ± 0.3 ‰and a δ^{18}O of 22.3 ± 0.3 ‰. In Kato et al. (1999) 3 cars with TWCs were measured, but only cold emissions were considered, since concentrations in the hot emissions were below their measurement threshold. These results are similar to the cold emissions found in this study.

Tsunogai et al. (2003), the only study available in which the cars (6 in total) were driven, found in some cases enrichment in δ^{13}C and variations in δ^{18}O a range similar to what was found here. This did not prevent them from giving a well-defined estimate of δ^{13}C and δ^{18}O , because the strongest deviations occurred for samples with low CO concentrations. For CO from petrol cars they reported δ^{13}C = -23.8 ± 0.8 ‰ and δ^{18}O = 25.3 ± ‰ and for diesel cars δ^{13}C = -19.5 ± 0.7 ‰ and δ^{18}O = -15 ± 1.0 ‰. I also found

Parameter	Overall	Idling	Cold petrol	Cold diesel	Parking garage
δ^{13}C (‰)	-28.7 ± 0.5	-29.6 ± 0.6	-29.8 ± 0.6	-22.3 ± 1.9	-29.5 ± 0.4
δ^{18}O (‰)	24.8 ± 0.3	25.3 ± 0.3	25.6 ± 0.2	17.1 ± 2.0	25.9 ± 0.4
H_2:CO (ppb:ppb)	0.71 ± 0.31	0.62 ± 0.29	0.45 ± 0.23	0.017 ± 0.018	0.46 ± 0.06
CO:CO_2 (ppb:ppm)	19.4 ± 6.8	51.2 ± 19.3	121.2 ± 43.4	14.1 ± 12.2	-
CH_4:CO_2 (ppb:ppm)	0.26 ± 0.05	0.59 ± 0.15	1.23 ± 0.29	0.22 ± 0.12	-

Table 8: All results found in this thesis for the car exhaust composition. Means of δ values are the weighted means, with the CO:CO_2 ratio as weight. Each gas ratio is computed as the ratio between the sum of the respective gas concentrations. For the parking garage samples the results from the Keeling plots (section 4.6) are used.

diesel cars to be higher in δ^{13}C and lower in δ^{18}O than petrol cars, but quantitatively the estimates deviate. Moreover, they found a positive correlation between δ^{18}O and δ^{13}C , similar to what we found for diesel cars. I did not find this correlation for petrol cars, which could reflect the increased complexity of CO regulation in petrol cars. For diesel cars these regulations don't have to be as extreme, because CO emissions are not as high.

I find an even wider spread in emissions than Tsunogai et al. (2003), suggesting emission regulations have grown increasingly complex. Additionally, different from Tsunogai et al. (2003), I also find depletion in δ^{13}C , but as Figure 18 reveals, these are the samples with the lowest CO concentrations. It could be that this is a new class of emissions not present or not measurable in 2003. Moreover, the same figure shows that when cold emissions are not considered, enrichment in δ^{13}C is found. In real-world emissions this middle class of δ^{13}C enriched emissions might be more important than this study suggests, because these correspond mostly to actual driving, which is probably more common than (cold) idling. In this aspect a more in-depth study of cars on a test bench could provide valuable insight.

The atmospheric studies mostly show agreement with these findings. Stevens et al. (1972) found a δ^{13}C close to fuel and a δ^{18}O of +17 to +23 ‰. Considering that the study was done in a time where chemistry in cars was still relatively simple, it makes sense that the values reflect their sources (fuel and air) relatively untouched. In Popa et al. (2014) (a tunnel study) enrichment in δ^{13}C of 3 ‰compared to δ^{13}C in fuel was found. This is similar to what Figure 18 shows for my middle class emissions.

I also found a connection between H_2:CO and δ^{13}C , in the form of a lower cut-off line, below which no samples were located. Vollmer et al. (2010) have shown that when the air-to-fuel ratio in petrol cars approaches stoichiometry, the H_2:CO increases, but only downstream of the catalyst. This indicates that a higher H_2:CO ratio corresponds to a more efficient catalyst, which is in line with the finding that the lowest CO emitters corresponded to the lowest δ^{13}C values. The weakness of the correlation suggests more is at work. It could be that catalytic efficiency is too simple a concept too explain the

full range of $\delta^{13}C$ variations. For example, variations in TWC temperature and the air-to-fuel ratio both affect the catalytic efficiency similarly, but might have a different effect on the fractionation of CO, since they lead to very different conditions under which CO is destroyed. A study of the isotopic fractionation of CO by a TWC in a lab study could provide valuable information on this subject.

5.2 CO_2 isotopes

In modern cars, effectively all carbon is emitted as CO_2. For this reason, the carbon isotopic composition of CO_2 from traffic is assumed to reflect that of fuel. Since oxygen also leaves the car as H_2O, and since CO_2 can equilibrate with H_2O through water-gas shift reactions, it is less certain what the $\delta^{18}O$ value in CO_2 from traffic is. It is generally considered that it reflects that of atmospheric oxygen (e.g. Cuntz et al. (2003)), but deviations from this assumption have been observed (Horvath et al. (2012); Schumacher et al. (2011)). These findings are in line with our results for petrol cars. However, for diesel cars we did find a constant $\delta^{18}O$ value for CO_2. A possible explanation is that in petrol cars, a significant amount of carbon is first emitted as non-CO_2 compounds and only later converted to CO_2 by the TWC, different from the more complete combustion in a diesel car. This could also explain why the $\delta^{18}O$ values of CO_2 from diesel cars are close to that of atmospheric oxygen.

Another interesting finding is that, for petrol cars, the range covered by $\delta^{18}O$ values of CO and $\delta^{18}O$ values of CO_2 is similar. Though the two are not correlated (Figure 12), the similarity in range indicates that they might be affected by the same processes. It is generally considered that CO does not equilibrate with H_2O though water-gas shift reactions, but it is uncertain whether this holds under the special conditions found in a TWC.

5.3 Gas ratios

Gas ratios are generally more widely studied than isotopic composition, in part because they are easier to measure and in part because they are known to a larger community. This means that whereas results for (CO) isotopes in this study greatly increase the available data on this subject, for gas ratios there are already quite some comprehensive studies.

Of the three gas ratios studied, CO:CO_2 is considered to be the most important, since CO emissions in urban areas are a problem. In this study I found that the ratio is highly variable. This is in line with the spread between existing studies. Generally, most recent studies agree on emissions of a few ppb:ppm (e.g. Vollmer et al. (2007); Bishop and Stedman (2008); Popa et al. (2014)). The CO:CO_2 value of 19.4 $\pm$ 6.4 ppb:ppm found in this study is higher. This is in line with the finding that our results might be biased towards conditions where CO emissions are high.

Interest in H_2:CO is similar to that in isotopes: atmospheric budgeting, in this case for H_2 emissions. Therefore, the available literature, though more extensive, is somewhat similar to that available on CO isotopes. Most studies namely involve atmospheric measurements, rather than measurements from individual cars. The H_2:CO ratio reported in most atmospheric studies (Yver et al. (2009); Hammer et al. (2009); Vollmer et al.

(2007); Aalto et al. (2009); Grant et al. (2010)) is in the range of 0.4 to 0.5 ppb:ppb. The results for the parking garage fit well into this array of estimates. More in-depth measurements on individual vehicles have also been done. In Vollmer et al. (2010) high variability in the ratio was found, dependent on the engine conditions. In Bond et al. (2010) the same variability was found. In both cases the best estimate differed significantly from the atmospheric studies: 0.25 and 1.02 ppb:ppb respectively. This shows that our best estimate 0.71 ± 0.31 is not far off from the atmospheric signal. Our low estimate of H_2:CO from diesel is in agreement with literature.

Data on CH_4:CO_2 emissions from cars is scarce, since they are deemed insignificant. This is confirmed in our study. We find emissions of approximately 72 μg CH_4/g CO_2. Even if all anthropogenic CO_2 emissions originate from traffic, a first estimate would put CH_4 emissions from traffic in the order of a few Tg. The global budget of CH_4 is in the order of several hundreds of Tg (e.g. Lelieveld et al. (1998)), so that even for this upper bound, CH_4 emissions from traffic are insignificant. The correlation between CO and CH_4 emissions for high emitters is interesting, since it might give information on the chemistry going on inside a car. It indicates that the processes responsible for producing and destroying CO and CH_4 are similar. However, since CH_4 emissions from traffic were found to be insignificant, a well-defined CO:CH_4 ratio from traffic cannot be used in atmospheric budgeting.

5.4 The reliability and representativeness of the sampling

For a wide range of samples it has been shown that the reproducibility is similar to what is expected from the measurement accuracy. However, it was also found that reproducibility of the sampling itself is very low. Two samples taken from the same car could have widely different compositions. The test bench measurements showed that indeed strong jumps in composition could occur for subsequent samples. Despite this finding, it is a complication that the results would be hard to reproduce. The low reproducibility is probably caused by the internal complexity of cars, which prevents reproducing the exact same internal state of a car each time it is sampled.

Another issue with the sampling in this study is that the distribution is arbitrary. The distribution is not representative of any standardized driving cycle. The data is also insufficient to provide an estimate of what these results would mean for a standard driving cycle. The reason we put confidence in our final weighted means is that even if the real-world distribution is different, the CSEEs would still be important. However, emissions from the samples, other than those of the 10 highest emitters, are not insignificant: they make up $\sim$ 20% of the total emissions in this study. It is therefore possible that they are more dominant in certain driving cycles. In fact, this is indeed what other literature indicates (see section 5.1).

Despite these difficulties, the approach used in this study is still very useful. Atmospheric measurements, or measurements of standardized driving cycles, are useful because they provide estimates of typical situations. However, these estimates are hard to extrapolate to different situations. Measurements of individual cars under specific driving conditions on the other hand, as taken in this study, provide estimates of the components (driving conditions and car characteristics) that all situations consist of. This is useful in studying different areas, where different driving conditions dominate, or where the traffic

fleet composition is different. Temporal evolutions, such an increase in the proportion of diesel cars (e.g. Eurostat, 2005[1]), can also be described using data from this type of study. Following that line of reasoning, these types of studies are valuable regardless of whether the sample distribution is representative of any driving cycle, since the aggregated results are not the most important part. However, for the bottom-up approach to be viable, the data obtained in this study is still insufficient.

5.5 Future research and emissions policies

Regardless of the reliability of the results found for the composition of car exhaust in this thesis, the results have strong implications for research into car exhaust in general. On the one hand it shows that determining a fleet average of traffic emissions from individual car measurements is a complex task. The spread that was found in the composition requires a large number of cars to be tested under a wide range of conditions. This is likely to get worse as emission regulation systems in cars become more complex.

If one is only interested in the traffic signature and not how it got to be that way, it might be easier to do integrated atmospheric measurements. The ease and accuracy of this approach makes it viable, even though it would have to be done separately for every individual fleet composition and driving condition (e.g. tunnels, highways, urban areas). On the other hand, in the interest of the mitigation of car emissions, the strong variability of the results emphasizes that this type of study can reveal the weak points in current emission regulation. An extension of the research done in this project could give even more insight as to which driving conditions dominate overall traffic emissions. Improving the optimal performance of TWCs might not reduce be the best approach, especially in urban areas, because it does not help in reducing CSEEs. However, in many cases this is the best way to comply with emission regulations, which mostly involve standardized tests.

Currently some randomly selected cars that leave the factory undergo standardized tests. There are certainly issues with these standardized tests (e.g. the Volskwagen scandal), but they at least study to some degree the impact of most driving conditions. The tests that cars have to undergo every few years after leaving the factory are far less stringent and insightful. For example, the APK test in the Netherlands only tests cars under stationary conditions (idling and revving). Moreover, the cars are driven to the test location by the owner, so that no CSEEs are measured. In another example, a study by TNO (Hensema et al., 2012) found that mopeds do not comply to standardized tests at all, even though they do undergo an emission test after leaving the factory. These examples show that current policies regarding traffic emissions may be inefficient: they would not catch deterioration of emissions if it only occurs under certain conditions.

For these reasons it is important that research into individual cars, which are actually being driven in the real world, continues. Isotopic research could help in the identifying which driving conditions and which types of cars are contributing the most, similar to how it was done in this study.

[1] `http://appsso.eurostat.ec.europa.eu/nui/submitViewTableAction.do`

6 Conclusions

In this study I investigated the composition of emissions from passenger cars. This was done in four approaches. Cars were sampled under idling conditions, when pressing down the accelerator without coupling (i.e. stationary) and on a testbench, where a full driving cycle was simulated. In the fourth approach atmospheric samples were taken in and near a number of parking garages. The main goal was to characterize the isotopic composition of CO in the exhaust and aggregate the results to an isotopic composition representative for CO from car emissions. The same was done for the gas ratios H_2:CO, CO:CO_2 and CH_4:CO_2. The final results are given in Table 8.

The results showed large spread in all parameters, seemingly preventing the computation of any fleet average. However, there were clear groups in the data that behaved distinctly. The main groups are cold diesel cars, cold petrol cars and hot cars. Cold diesel cars behaved as a very well-defined group for all parameters, but were not found to contribute significantly to the gas ratios investigated in this study. Most cold petrol cars behaved as a distinct group. These cars where characterized by high CO and CH_4 emissions, a nearly constant isotopic composition of CO and a constant H_2:CO ratio. Hot cars, both diesel and petrol, were the cars that showed the highest spread in isotopic composition and in the H_2:CO ratio, while generally CO:CO_2 and CH_4:CO_2 ratios were low. In the overall data, the spread on all parameters was huge: for δ^{13}C 0 to -60 ‰, for δ^{18}O $\sim$ +20 to +35 ‰and for all gas ratios several orders of magnitude. A Welch's t-test was performed to distinguish between hot and cold petrol cars. They were found to form two significantly different groups for H_2:CO, CH_4:CO_2, CO:CO_2 and for δ^{13}C , but not for δ^{18}O .

Combining these groups in an overall isotopic composition of CO through a mean, weighted by the CO:CO_2 ratio, gave a surprisingly well-defined ratio. The δ^{13}C value is close to that of fuel and the δ^{18}O value enriched compared to atmospheric oxygen. This composition is in agreement with the traffic signature derived from the parking garage samples. The most recent studies reported δ^{13}C values slightly more enriched. The isotopic values were dominated by the group of samples with the highest concentrations, all taken from cold, idling petrol cars. It is unclear whether this extremely high contribution from a small set of samples is a bias in this study, or a reflection of the importance of a few moments of high emissions (mostly CSEEs) to total traffic emissions. The good agreement with the atmospheric signature in the parking garage samples suggests the latter. However, the enriched δ^{13}C values reported in literature suggest the importance of CSEEs might be overestimated in this study.

The H_2:CO ratio that was found in the individual car measurements did not differ significantly from the values reported in literature. The H_2:CO ratio was also dominated by the high emitters, but to a lesser degree, since samples with low CO concentrations sometimes still showed significant H_2 emissions. It is therefore likely that to determine an accurate H_2:CO ratio from individual car measurements, one does have to consider a sample distribution somewhat representative for real-world driving cycles. The ratio found in the parking garage measurements was in close agreement with literature.

Results for the CO:CO_2 ratio were less coherent than those for the H_2:CO ratio. The spread in the results spanned 7 orders of magnitude. This highlights the importance for CSEEs in modern cars, since all of the high emitters were cold petrol cars.

CH_4 emissions were dominated by the same high emitters. The results in this study support the finding in previous studies that CH_4 emissions from cars are insignificant in the overall CH_4 budget.

Three different petrol cars were tested on the testbench. These measurements revealed that the variations between cars found in the idling measurements were also found within individual cars, when driving conditions were varied. The only general behaviour that held for each car was that CO and CH_4 emissions were slightly elevated at a speed of 120 km/h. However, these emissions were still several orders of magnitude smaller than the highest cold car emissions. In all other aspects the cars were found to behave differently, so that no general behaviour could be defined.

The various parameters showed some correlations. The H_2:CO ratio was found to be weakly negatively correlated to the δ^{13}C values. This correlation was most obvious in a lower cut-off, below which very few samples were found. This means that only two samples (out of 126) had both a low H_2:CO ratio and a depleted δ^{13}C value. Previous research showed that the H_2:CO sharply increases towards an air-to-fuel ratio of 1. The correlation found here suggests that this is the same condition for which the most depleted δ^{13}C values are found.

For both the high-CO petrol samples and the diesel samples a strong correlation between CO:CO_2 and CH_4:CO_2 was found, showing that the processes affecting these two gases are to some degree similar. The spread on this correlation for hot petrol cars was again large. For the diesel samples a strong positive correlation between δ^{18}O and δ^{13}C in CO was found. The exact cause of this correlation remains unclear.

The samples taken near and in parking garages showed at times strongly elevated CO and H_2 concentrations. Keeling plots of the data resulted in a well-defined traffic signature for δ^{13}C , δ^{18}O and H_2:CO, all of which are given in Table 8. These values were similar to both literature and to the weighted means of the individual car measurements. This confirms that in these parking garages the high emitters dominate.

For a selected set of samples the isotopic composition of CO_2 was also determined. The δ^{13}C values were found to be within a range of 2 ‰, where most spread came from differences between cars. This reflects the slight differences in isotopic composition between different oil sources. δ^{13}C values of diesel and petrol cars were found to be similar. The δ^{18}O values in CO_2 of petrol cars were found to vary between 20 and 35 ‰, similar to the δ^{18}O values of CO. These two δ^{18}O values were not correlated. For diesel cars the δ^{18}O in CO_2 was found to be vary in a range of 1 ‰around +23 ‰: the δ^{18}O of atmospheric oxygen.

Overall, the spread in the results showed that a bottom-up estimate of car emissions is complex and might be dominated by a small number of cars and driving conditions. Studies where results from a handful of cars are extrapolated to an entire fleet should therefore be considered with caution. A comprehensive study of a wide array of cars measured under a wide range of conditions could provide valuable information on the best methods for reducing pollutant emissions.

References

T Aalto, M Lallo, J Hatakka, and T Laurila. Atmospheric hydrogen variations and traffic emissions at an urban site in finland. *Atmospheric Chemistry and Physics*, 9 (19):7387–7396, 2009.

Jonas Andersson, Matilda Antonsson, Lisa Eurenius, Eva Olsson, and Magnus Skoglundh. Deactivation of diesel oxidation catalysts: Vehicle-and synthetic aging correlations. *Applied Catalysis B: Environmental*, 72(1):71–81, 2007.

Robert J Andres, GREGG Marland, T Boden, and STEVE Bischof. Carbon dioxide emissions from fossil fuel consumption and cement manufacture, 1751-1991; and an estimate of their isotopic composition and latitudinal distribution. Technical report, Oak Ridge National Lab., TN (United States); Oak Ridge Inst. for Science and Education, TN (United States), 1994.

P Bielaczyc, A Szczotka, and J Woodburn. The effect of a low ambient temperature on the cold-start emissions and fuel consumption of passenger cars. *Proceedings of the Institution of Mechanical Engineers, Part D: Journal of Automobile Engineering*, 225 (9):1253–1264, 2011.

Gary A Bishop and Donald H Stedman. A decade of on-road emissions measurements. *Environmental Science & Technology*, 42(5):1651–1656, 2008.

SW Bond, R Alvarez, MK Vollmer, M Steinbacher, M Weilenmann, and S Reimann. Molecular hydrogen (h 2) emissions from gasoline and diesel vehicles. *Science of the total environment*, 408(17):3596–3606, 2010.

CAM Brenninkmeijer, T Röckmann, M Bräunlich, P Jöckel, and P Bergamaschi. Review of progress in isotope studies of atmospheric carbon monoxide. *Chemosphere-Global Change Science*, 1(1):33–52, 1999.

Carl AM Brenninkmeijer and Thomas Röckmann. Principal factors determining the 18o/16o ratio of atmospheric co as derived from observations in the southern hemispheric troposphere and lowermost stratosphere. *Journal of Geophysical Research: Atmospheres*, 102(D21):25477–25485, 1997.

Paul J Crutzen and Peter H Zimmermann. The changing photochemistry of the troposphere. *Tellus B*, 43(4):136–151, 1991.

Matthias Cuntz, Philippe Ciais, Georg Hoffmann, and Wolfgang Knorr. A comprehensive global three-dimensional model of δ18o in atmospheric co2: 1. validation of surface processes. *Journal of Geophysical Research: Atmospheres*, 108(D17), 2003.

H Christopher Frey, Alper Unal, Nagui M Rouphail, and James D Colyar. On-road measurement of vehicle tailpipe emissions using a portable instrument. *Journal of the Air & Waste Management Association*, 53(8):992–1002, 2003.

Ulrike Gamnitzer, Ute Karstens, Bernd Kromer, Rolf EM Neubert, Harro AJ Meijer, Hartwig Schroeder, and Ingeborg Levin. Carbon monoxide: A quantitative tracer for fossil fuel co2? *Journal of Geophysical Research: Atmospheres*, 111(D22), 2006.

A Grant, KF Stanley, SJ Henshaw, DE Shallcross, and S O'Doherty. High-frequency urban measurements of molecular hydrogen and carbon monoxide in the united kingdom. *Atmospheric Chemistry and Physics*, 10(10):4715–4724, 2010.

Hui Guo, Qing-yu Zhang, Yao Shi, Da-hui Wang, Shu-ying Ding, and Sha-sha Yan. Characterization of on-road co, hc and no emissions for petrol vehicle fleet in china city. *Journal of Zhejiang University Science B*, 7(7):532–541, 2006.

Samuel Hammer, Felix Vogel, Markus Kaul, and Ingeborg Levin. The h2/co ratio of emissions from combustion sources: comparison of top-down with bottom-up measurements in southwest germany. *Tellus B*, 61(3):547–555, 2009.

Amber Hensema, Pim van Mensch, Robin Vermeulen, and H Baarbé. *Tail-pipe emissions and fuel consumption of standard and tampered mopeds*. Delft: TNO, 2012.

B Horvath, MEG Hofmann, and A Pack. On the triple oxygen isotope composition of carbon dioxide from some combustion processes. *Geochimica et Cosmochimica Acta*, 95:160–168, 2012.

Shungo Kato, Hajime Akimoto, Maya Bräunlich, Thomas Röckmann, and Carl AM Brenninkmeijer. Measurements of stable carbon and oxygen isotopic compositions of co in automobile exhausts and ambient air from semi-urban mainz, germany. *Geochemical journal*, 33(2):73–77, 1999.

JOS Lelieveld, Paul J Crutzen, and Frank J Dentener. Changing concentration, lifetime and climate forcing of atmospheric methane. *Tellus B*, 50(2):128–150, 1998.

D Ludykar, R Westerholm, and J Almen. Cold start emissions at+ 22,- 7 and- 20 c ambient temperatures from a three-way catalyst (twc) car: regulated and unregulated exhaust components. *Science of the Total Environment*, 235(1):65–69, 1999.

EK Nam, TE Jensen, and TJ Wallington. Methane emissions from vehicles. *Environmental science & technology*, 38(7):2005–2010, 2004.

SL Pathirana, C van der Veen, ME Popa, and T Röckmann. An analytical system for studying the stable isotopes of carbon monoxide using continuous flow-isotope ratio mass spectrometry (cf-irms). *Atmospheric Measurement Techniques Discussions*, 8(2): 2067–2092, 2015.

Luc Pelkmans and Patrick Debal. Comparison of on-road emissions with emissions measured on chassis dynamometer test cycles. *Transportation Research Part D: Transport and Environment*, 11(4):233–241, 2006.

Maria Elena Popa, AT Vermeulen, WCM van den Bulk, PAC Jongejan, AM Batenburg, W Zahorowski, and T Röckmann. H 2 vertical profiles in the continental boundary layer: measurements at the cabauw tall tower in the netherlands. *Atmospheric chemistry and physics*, 11(13):6425–6443, 2011.

Maria Elena Popa, MK Vollmer, Armin Jordan, Willi A Brand, SL Pathirana, Michael Rothe, and T Röckmann. Vehicle emissions of greenhouse gases and related tracers from a tunnel study: Co: Co 2, n 2 o: Co 2, ch 4: Co 2, o 2: Co 2 ratios, and the stable isotopes 13 c and 18 o in co 2 and co. *Atmospheric Chemistry and Physics*, 14 (4):2105–2123, 2014.

T Röckmann, P Jöckel, Valérie Gros, M Bräunlich, G Possnert, and CAM Brenninkmeijer. Using 14 c, 13 c, 18 o and 17 o isotopic variations to provide insights into the high northern latitude surface co inventory. *Atmospheric Chemistry and Physics*, 2(2): 147–159, 2002.

M Schumacher, RA Werner, HAJ Meijer, HG Jansen, Willi A Brand, H Geilmann, and REM Neubert. Oxygen isotopic signature of co 2 from combustion processes. *Atmospheric Chemistry and Physics*, 11(4):1473–1490, 2011.

CM Stevens, L Krout, Dr Walling, A Venters, A Engelkemeir, and LE Ross. The isotopic composition of atmospheric carbon monoxide. *Earth and Planetary Science Letters*, 16 (2):147–165, 1972.

Urumu Tsunogai, Yosuke Hachisu, Daisuke D Komatsu, Fumiko Nakagawa, Toshitaka Gamo, and Ken-ichi Akiyama. An updated estimation of the stable carbon and oxygen isotopic compositions of automobile co emissions. *Atmospheric Environment*, 37(35): 4901–4910, 2003.

Martin K Vollmer, Niklas Juergens, Martin Steinbacher, Stefan Reimann, Martin Weilenmann, and Brigitte Buchmann. Road vehicle emissions of molecular hydrogen (h 2) from a tunnel study. *Atmospheric Environment*, 41(37):8355–8369, 2007.

MK Vollmer, S Walter, SW Bond, P Soltic, and T Röckmann. Molecular hydrogen (h 2) emissions and their isotopic signatures (h/d) from a motor vehicle: implications on atmospheric h 2. *Atmospheric chemistry and physics*, 10(12):5707–5718, 2010.

Martin Weilenmann, Patrik Soltic, Christian Saxer, Anna-Maria Forss, and Norbert Heeb. Regulated and nonregulated diesel and gasoline cold start emissions at different temperatures. *Atmospheric environment*, 39(13):2433–2441, 2005.

Martin Weilenmann, Jean-Yves Favez, and Robert Alvarez. Cold-start emissions of modern passenger cars at different low ambient temperatures and their evolution over vehicle legislation categories. *Atmospheric environment*, 43(15):2419–2429, 2009.

Martin Weiss, Pierre Bonnel, Rudolf Hummel, Alessio Provenza, and Urbano Manfredi. On-road emissions of light-duty vehicles in europe. *Environmental science & technology*, 45(19):8575–8581, 2011.

C Yver, M Schmidt, P Bousquet, W Zahorowski, and M Ramonet. Estimation of the molecular hydrogen soil uptake and traffic emissions at a suburban site near paris through hydrogen, carbon monoxide, and radon-222 semicontinuous measurements. *Journal of Geophysical Research: Atmospheres*, 114(D18), 2009.

A Pressure calibration

Most car samples require many dilutions, which makes it important to work with an accurate pressure sensor. To quantify the uncertainty of the Keller LEO2 sensor and to determine if its behaviour is linear, I calibrated it against a high-precision pressure sensor (Paroscientific, model 745). The high-precision sensor measures pressures up to 1 bar with an error < 0.08 mbar.

For the calibration a flask at atmospheric pressure was connected to a system of stainless steel tubes, to which the pressure sensors were also connected. Connected to the same system through a switch valve was a vacuum pump. This set-up allowed for continuous detection of the pressure with all sensors, while the pressure in the flask could be reduced stepwise by opening the valve connecting the vacuum pump.

The results are shown in Figure 19. It turned out the simple pressure sensor detected a pressure which decreased in approximately the same way as that measured by the high-precision sensor. There was however a continuous offset. To determine this offset two linear fits with slope 1 were made between the high-precision and the two simple sensor results. This showed the LEO2 had an average offset of 0.71 mbar. Correcting with this offset lead to an average residual error in LEO2 results of 0.36 mbar. The behaviour of the pressure sensor was found to be similarly linear above 1 bar.

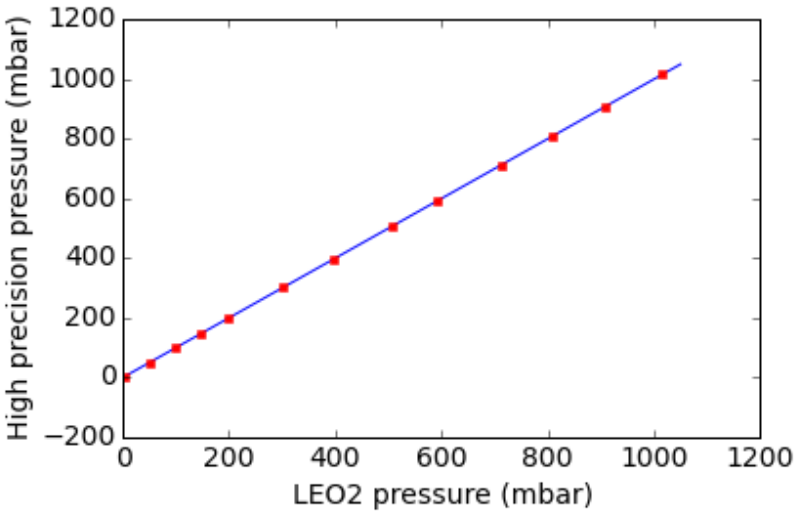

Figure 19: The pressures that were measured after each step with the different sensors. The high-precision pressures are on the y-axis and those for LEO2 on the x-axis. A linear fit with slope 1 is given by the blue line.

B Instrumental reproducibility

Every measurement instrument has its errors. Propagating these errors through the data analysis gives the analytical errors in the end result. To test whether these errors are realistic, a number of sample back-ups were measured. The difference between the

back-ups and the originals should be similar to the analytical errors in the samples. In addition, since back-ups were generally measured weeks later than the original, stability of the flask's composition on this timescale was also tested.

In total 12 pairs of samples were analysed for both gas concentrations and CO isotopic composition and 23 were analysed only for CO isotopic composition. The results are given in Table 9. The reproducibility is taken as the mean relative difference between the two samples in a pair. The analytical error was found by propagating the relative analytical errors of the two samples through: $\sqrt{\sigma_a^2 + \sigma_b^2}$. The values given are the average of the errors of the two points in each pair. In general good agreement is found. The CH_4 errors seem to be overestimated in the analytical approach. However, the analytical errors were not adjusted, because the spread in errors is large and the deviations between the reproducibility and the analytical error are not significant.

Parameter	**Reproducibility**	**Analytical error**
δ^{13}C (‰)	0.17	0.14
δ^{18}O (‰)	0.29	0.28
H_2 (%)	5.1	4.3
CO (%)	6.0	4.1
CO_2 (%)	3.4	3.2
CH_4 (%)	13.5	23.7

Table 9: The reproducibility determined from the differences between results from back-ups and originals for each parameter, along with the analytical error, which is calculated through propagation of the instrumental errors.

For the isotopic composition the analytical error is based on the error reported by Pathirana et al. (2015): 0.1 ‰ and 0.2 ‰ for δ^{13}C and δ^{18}O respectively. The results found in this paragraph show that the actual error is very similar to the the propagated analytical error: 0.17 ‰and 0.29 ‰ for δ^{13}C and δ^{18}O respectively. An error of 0.2 and 0.3 ‰ for δ^{13}C and δ^{18}O respectively is adopted in the rest of the thesis.

C RGA non-linearity

The reduced gas analyser (RGA) used for CO and H_2 measurements is known to behave non-linearly, especially at high concentrations. A test was done to determine the extent of the non-linear behaviour and to determine the best method to deal with it. The non-linear behaviour is caused by the detection method. The degree to which additionally released Hg reduces the UV light, depends on the amount of UV light: evidently UV light can't be reduced by more than the starting intensity of the lamp. Moreover, above a certain concentration all HgO will have reacted, leading to flat-top peaks for high concentrations. The sensitivity of the RGA is different for H_2 and CO, so that they will require separate

fits. Non-linearity measurements were done at two points in time in between which the UV lamp inside the RGA was switched. The first time only CO was measured and the second time also H_2 was measured.

I reduced the concentration in the sample so that is was just measurable on the RGA. I then diluted the concentration in the flask in steps and measured the sample in between dilutions on the RGA. For the analysis the concentration in the flask when it was closest to the reference was computed. From this value and the pressure data, the concentration after each dilution was computed. This was compared with the corrected peak value $I_{\text{cor}} = \frac{I_{\text{meas}}}{I_{\text{ref}}} * I_{\text{ref,mean}}$. This correction removes the influence of variations in RGA sensitivity during measurements. The results are shown in Figure 20.

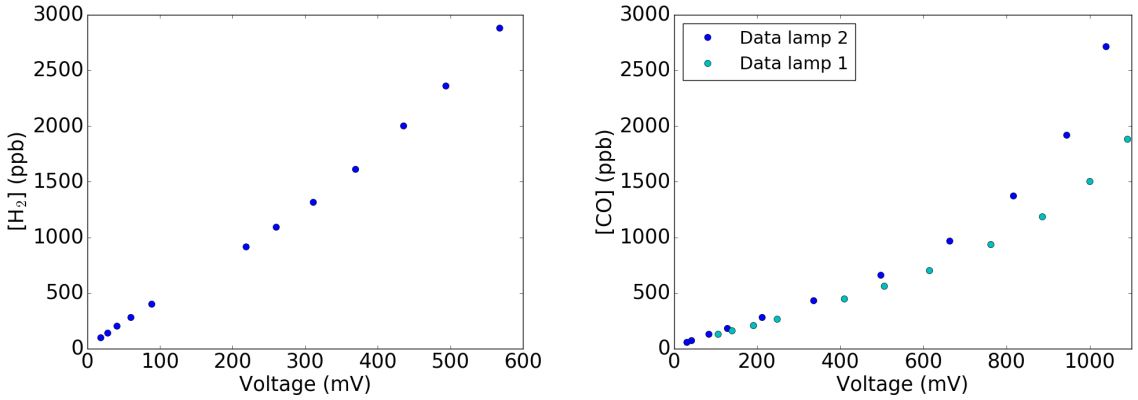

(a) The results for H_2.

(b) The results for CO.

Figure 20: The results for the non-linearity tests. Concentration in the flasks, as determined from the dilutions, are plotted against the corresponding peak heights.

Clearly the RGA behaves strongly non-linearly for high concentrations. However, at low concentrations the behaviour is still non-linear enough to merit a correction. This correction will focus on the regime below 500 mV, since this is the regime in which measurements were done.

The sensitivity of the RGA shifts through time and with temperature, so that making a correction that works consistently is not straightforward. The correction used in this thesis is based on the observation that though the absolute sensitivity shifts, the relative sensitivity does not. If at one point 100 mV corresponds to 100 ppb and 200 mv to 250 ppb and at another 100 mV corresponds to 200 ppb, then 200 mV will corresponds to 500 ppb. Therefore I determined the sensitivity at each voltage relative to the arbitrarily chosen 500 mV, the results of which are shown in Figures 21.

The results even for the two different lamps for CO follow roughly the same curve, demonstrating that relative sensitivity is indeed quite constant. For H_2 only one dataset is available, but we can assume that the same holds there. Since the sensitivity at the peak height of both the reference and the sample is known, determining the absolute concentration in the sample is straightforward. From the spread around the non-linearity curve for CO the uncertainty in the correction is estimated as 1%.

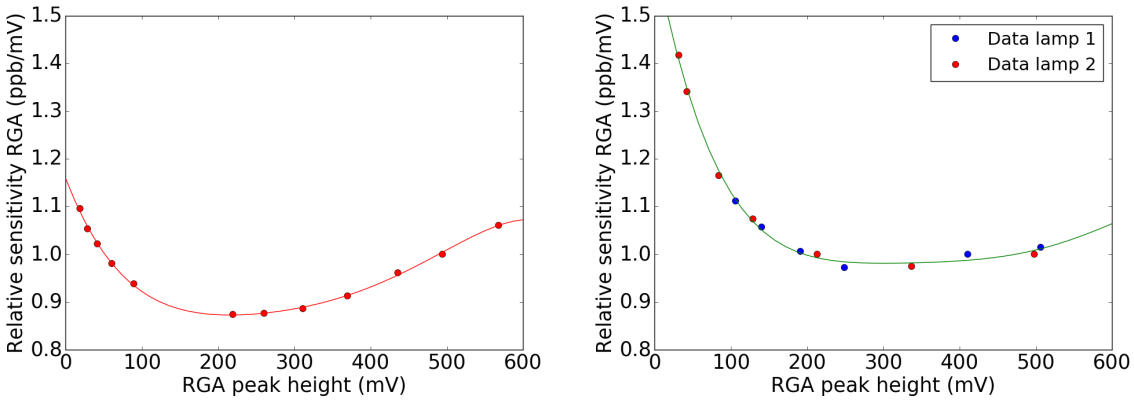

(a) The correction for H_2.

(b) The correction for CO.

Figure 21: The non-linearity correction for the sensitivity of the RGA (relative to 500 mV) at different peak heights for H_2 and CO. Measurements on the non-linearity of CO were done twice, for two different lamps, whereas for H_2 they were done once.

D Keeling plot for H_2:CO

A Keeling plot is commonly used in isotope studies to determine the source values from a series of measurements of varying contamination. The derivation of the equation used for a Keeling plot of δ^{13}C is given in section 4.6. However, using this same concept for gas ratios, as was done in the same section, is not so common. Since the derivation goes somewhat differently and is not commonly used, it is given in this appendix.

Consider a constant background H_2:CO ratio r_{bg} and a constant car ratio r_{car};. The total atmospheric H_2:CO ratio r_{atm} is then given by:

$$r_{atm} = \frac{[H_2]_{bg} + [H_2]_{car}}{[CO]_{bg} + [CO]_{car}}, \tag{7}$$

or:

$$[CO]_{atm} r_{atm} = r_{bg}[CO]_{bg} + r_{car}[CO]_{car}. \tag{8}$$

This is of the same form as equation 5, with r replacing δ^{13}C . It can be similarly rewritten to:

$$r_{atm} = (r_{bg} - r_{car})\frac{[CO]_{bg}}{[CO]_{atm}} + r_{car}. \tag{9}$$

This again gives a linear relation, this time between r_{atm} and $[CO]^{-1}_{atm}$, with r_{car} as the y-axis intercept.

E Supplementary figures

In this Appendix the results for the year of manufacture (Figure 22) and mileage (Figure 23 are presented. In the figures, the various emission parameters are plotted against

these two parameters. Only the idling results are included, to minimize the influence from driving conditions. Additionally, these were the samples that involved a wide variety of cars. As is mentioned in section 4.1, no correlations were found. This is likely because the sample size is too small and not uniformly distributed. From newer cars one would expect lower emissions, but since the newest cars sampled were also generally cold cars, this is not necessarily expected for our results.

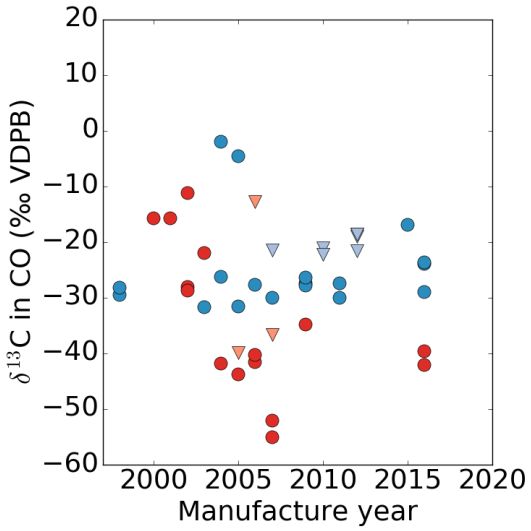

(a) δ^{13}C vs. the year of manufacture.

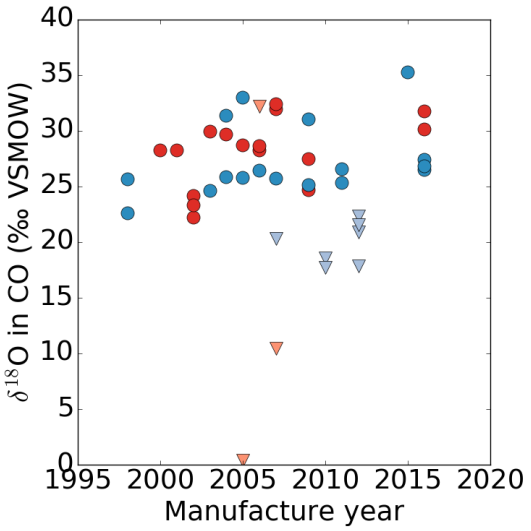

(b) δ^{18}O vs. the year of manufacture.

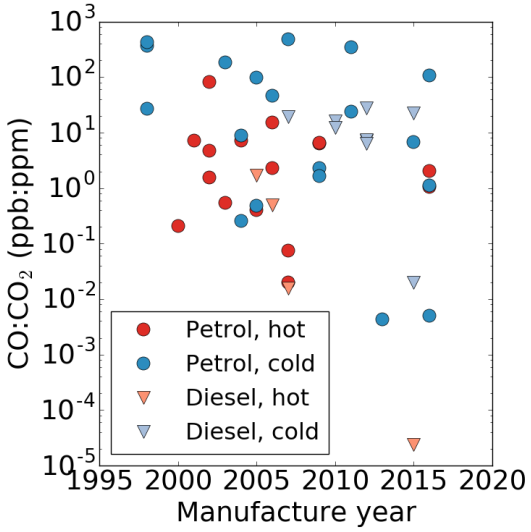

(c) CO:CO_2 vs. the year of manufacture.

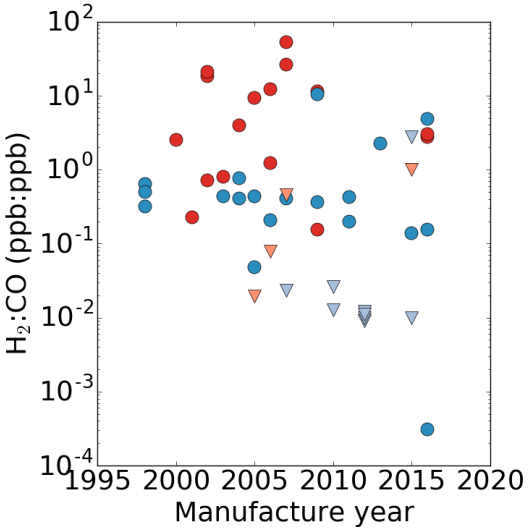

(d) H_2:CO vs. the year of manufacture.

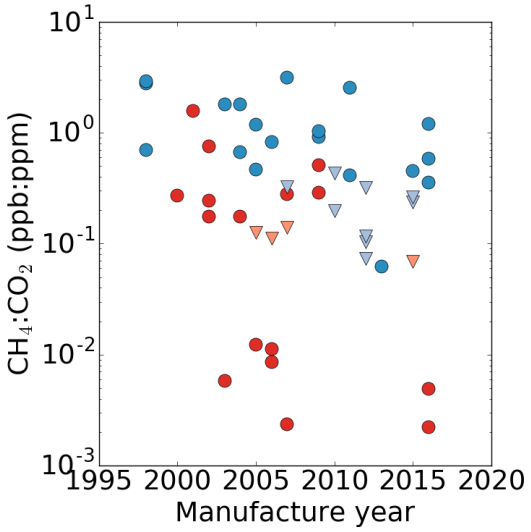

(e) CH_4:CO_2 vs. the year of manufacture.

Figure 22: The results for the various emission parameters plotted against the year of manufacture of each car. Only the idling samples are included.

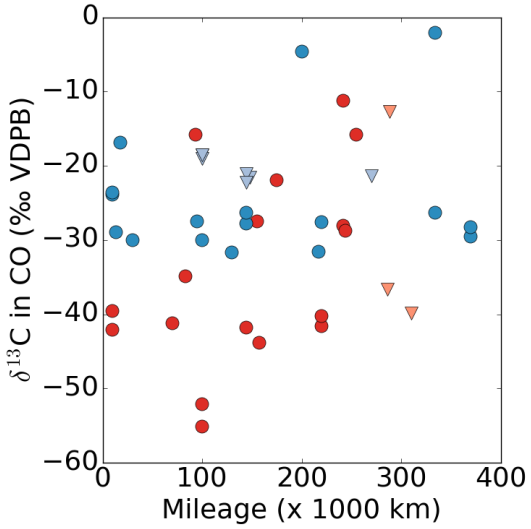

(a) δ^{13}C vs. mileage.

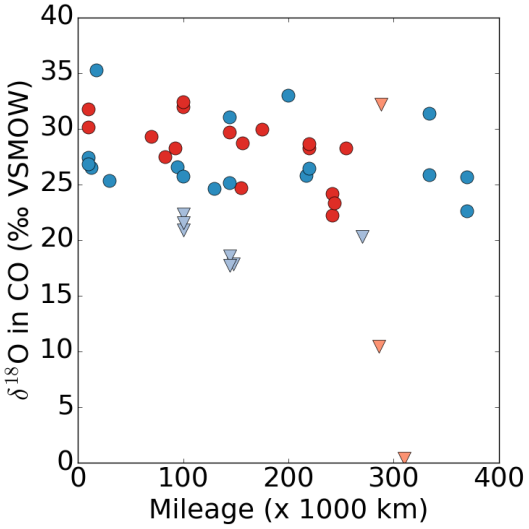

(b) δ^{18}O vs. mileage.

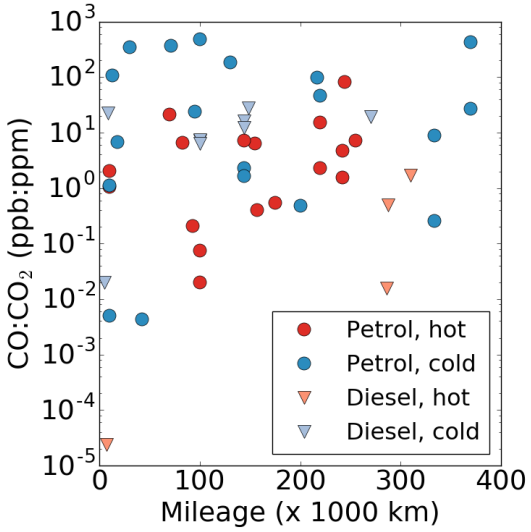

(c) CO:CO_2 vs. mileage.

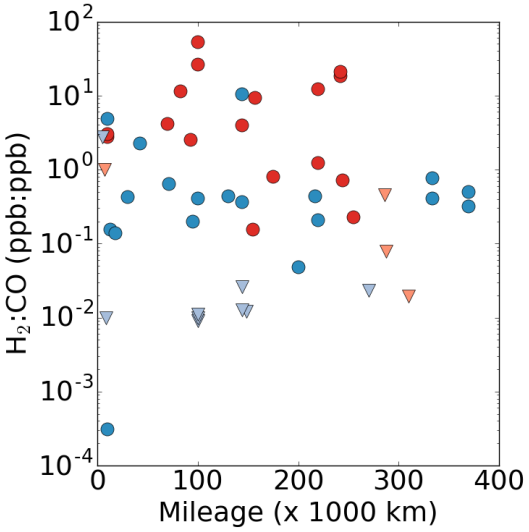

(d) H_2:CO vs. mileage.

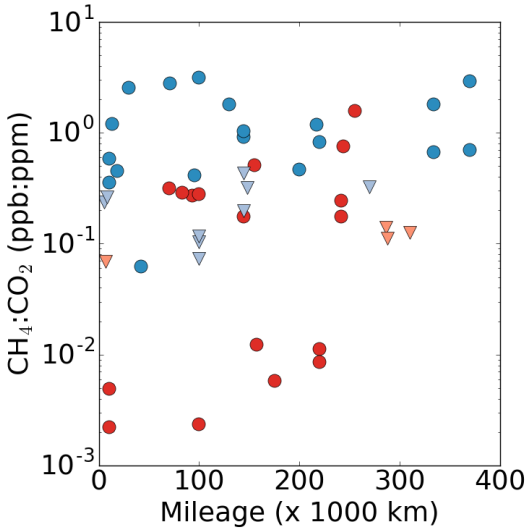

(e) CH_4:CO_2 vs. mileage.

Figure 23: The results for the various emission parameters plotted against the mileage of each car. Only the idling samples are included.